

Decoupling and Depinning II: Flux lattices in disordered layered superconductors

Baruch Horovitz

*Department of Physics and Ilze Katz center for nanotechnology,
Ben-Gurion University of the Negev, Beer-Sheva 84105, Israel*

Phase transitions of a flux lattice in layered superconductors with magnetic field perpendicular to the layers and in presence of disorder are studied. We find that disorder generates a random Josephson coupling between layers which leads to a Josephson glass (JG) phase at low temperatures; vanishing of the JG order identifies a depinning transition. We also find that disorder and thermal fluctuations lead to layer decoupling where the renormalized Josephson coupling vanishes. Near decoupling an anharmonic regime is found, where usual elasticity and the resulting Bragg glass are not valid. The depinning line crosses the decoupling line at a multicritical point, resulting in three transition lines and a crossover line. The phase diagram is consistent with the unusual data on $Bi_2Sr_2CaCu_2O_8$ such as the "second peak" and depinning transitions. The Josephson plasma frequency is evaluated in the various phases.

PACS numbers: 74.25.Qt, 74.25.Dw, 74.50.+r

I. INTRODUCTION

The phase diagram of layered superconductors in a magnetic field B perpendicular to the layers is of considerable interest in view of extensive experiments on high temperature superconductors¹. A first order transition in $YBa_2Cu_3O_7$ (YBCO) and in $Bi_2Sr_2CaCu_2O_8$ (BSCCO) has been interpreted as a melting transition of the flux lattice. This first order transition terminates at a multicritical point, which for BSCCO^{2,3} is at $B_0 \approx 300 - 10^3 G$ and $T_0 \approx 40 - 50 K$, while for YBCO⁴ it is at $B_0 \approx 2 - 10 T$ and $T_0 \approx 60 - 80 K$, depending on disorder and oxygen concentration. The multicritical point also terminates a "second peak" transition^{1,2,3,4} which is manifested by a sharp increase in magnetization and in critical current. The transition line at $B \approx B_0$ and $T < T_0$ is weakly T dependent and was found to be smoothly connected with the first order line⁵. Neutron scattering and μ SR data^{1,6} show that positional correlations of the flux lattice are significantly reduced near these phase boundaries, except however, near the multicritical point where a reentrant behavior is observed⁷. Data on $Nd_{1.85}Ce_{0.15}CuO_{4-\delta}$ (NCCO) has also shown a second peak transition; here, however, B_0 decreases with temperature near the superconducting transition at $T_c \approx 23 K$ with no apparent multicritical point⁸. The second peak phenomena is also pronounced in other layered systems such as $NbSe_2$ ^{9,10} and in Pb/Ge multilayers¹¹. Recent decoration data¹² on $NbSe_2$ has shown that the topology of the vortex structure is weakly affected by the second peak transition. Hence the nature of the phase at $B > B_0$ is not well established.

The Josephson plasma resonance is a probe of the Josephson coupling^{13,14} and can be used to probe the various phase transitions. Recent data on BSCCO has indeed shown a significant reduction in the resonance frequency at the second peak transition^{15,16}.

In a remarkable experiment Fuchs et al.¹⁷ have shown that the phase diagram of BSCCO is much more elaborate. They show that the spatial distribution of an external current exhibits a transition from bulk pinning to surface pinning of vortices with most of the current flowing at the sample edges. This depinning line crosses the multicritical point and its temperature is almost B independent at $B < B_0$. The depinning transition correlates with anomalies in vibrating reed experiments¹⁸ and in magnetization¹⁹. Thus there are four transition lines which emanate from the multicritical point at B_0, T_0 : The first order line, the second peak line and depinning lines for both $B < B_0$ and $B > B_0$.

The notion of vortex matter in the presence of disorder has emerged as a fundamental problem of elastic manifolds in a random media²⁰. This has motivated an extensive theoretical effort towards understanding the field-temperature ($B - T$) phase diagram in presence of disorder. Impurity disorder does not allow long range translational order of the flux lattice and finite domains are expected²¹. At low temperatures and fields the system is a Bragg glass^{22,23}, i.e. the lattice is dislocation free, at long scales the displacement correlations decay as a power law and Bragg peaks are expected. The impurity induced domains are essential for the description of both equilibrium, e.g. thermodynamic phase transitions and non-equilibrium, e.g. critical current phenomena. Melting, e.g., is expected to occur by thermal or disorder induced dislocations, as indeed demonstrated for fields parallel to the layers^{24,25}. Numerical simulations on related XY models have also shown disorder induced melting^{26,27,28}.

The flux lattice can undergo a transition which is unique to layered superconductors, i.e. a decoupling transition^{29,30}. In this transition the Josephson coupling between layers vanishes while the lattice is maintained by the electro-magnetic coupling between layers. A disorder induced decoupling was also proposed as a crossover phenomena³¹. Decoupling

in presence of columnar defects was also studied³², showing enhancement of the coupled phase.

It has been shown that decoupling coalesces with a defect unbinding transition^{33,34} which has analogs in isotropic systems³⁵. The resulting vacancies and interstitials lead to a reduction in the elastic tilt modulus³⁶, consistent with the decoupling scenario as described below. It is possible then that a decoupling-defect transition accounts for the peak phenomena in all type II superconductors. The analysis below is, however, presented for layered anisotropic systems where quantitative predictions can be made. Vacancies and interstitials are neglected; their role is discussed in the concluding section of the preceding companion article³⁷.

In the present work we expand our previous work^{38,39} and study effects of disorder at temperatures below the melting temperature T_m by employing replica symmetry breaking (RSB) methods. The most interesting finding is that of a glass order parameter which we term as Josephson glass (JG), as it is due to disorder induced on the Josephson coupling. The JG order is expected to lead to stronger pinning, hence the line where JG vanishes is associated with a depinning line. We find that the JG and decoupling lines cross and lead to four distinct phases which meet at one point in the $B - T$ phase diagram, remarkably close to the experimental phase diagram¹⁷. This paper follows a companion one³⁷ where the decoupling transition is studied in the pure system by second order renormalization group (RG).

The full problem addressed here involves the following set of nonlinearities: (i) Josephson coupling which involves both pancake displacements and a nonsingular phase. (ii) A disordered Josephson coupling which leads to the JG order. (iii) A nonlinear coupling of disorder to the displacement pattern, leading to the well studied Bragg glass (BG)^{22,23}. After presenting the model in section II, we study in section III a simplified version of the full problem in which the nonsingular phase is neglected and also the disorder coupling is linearized, corresponding to scales within finite domains. These approximations lead to an unphysical divergence of an integral $I(z)$ where z is the renormalized Josephson coupling, i.e. $z \rightarrow 0$ at decoupling. In section III we assume that $I(z)$ is convergent and behaves as $\sim \ln z$, an assumption that is justified in appendices A, B and C. In appendix A we extend section III to solve the combined BG/JG system, though the nonsingular phase is neglected. In appendix B the BG system including the non-singular phase is solved, but JG is neglected, as relevant to thermal decoupling. In both appendices A and B we find an additional $\ln^2 z$ term which signals a divergence of disorder effects in a regime close to decoupling. In appendix C we study JG with the nonsingular phase, but disorder is linearized. It is shown that $I(z)$ converges even in this situation, while an additional $1/\sqrt{z}$ term is generated. In section IV we present a dimensional derivation of domain sizes which correctly reproduces the pinning and BG lengths. Near decoupling there is a regime of nonlinear elasticity with an apparent jump of the tilt modulus c_{44} and the critical current. This anharmonic regime coincides with the onset of the $\ln^2 z$ term in appendices A, B. In section V the Josephson plasma frequency is studied, being an efficient probe for identifying the various phases. In section VI we discuss available data on the second peak and depinning transitions. We propose that decoupling accounts for the main features of the second peak transition while the depinning transitions correspond to the onset of JG order.

II. THE MODEL

Consider a flux lattice with an equilibrium position of the l -th flux line at vectors \mathbf{R}_l of a regular two-dimensional lattice. The flux line is composed of a sequence of singular points, or "pancake" vortices, whose positions at the n -th layer can fluctuate to $\mathbf{R}_l + \mathbf{u}_l^n$. Of particular interest is the transverse part of \mathbf{u}_l^n with the Fourier transform $u_T(\mathbf{q}, k)$, where \mathbf{q}, k are wavevectors parallel and perpendicular to the layers, respectively. The elastic energy due to the electromagnetic coupling has the form

$$\mathcal{H}_{e-m} = \frac{1}{2} \sum_{\mathbf{q}, k} (da^2)^2 [c_{66}^0 q^2 + c_{44}^0(k) k_z^2] |u_T(\mathbf{q}, k)|^2 \quad (1)$$

where the flux line density is $1/a^2$, d is the spacing between layers, \mathbf{q} is within the Brillouin zone [of area $(2\pi/a)^2$], $|k| < \pi/d$ and $k_z = (2/d) \sin(kd/2)$. The shear and tilt moduli are given (for $a \gg d$) by^{40,41,42}

$$\begin{aligned} c_{66}^0 &= \tau / (16da^2) \\ c_{44}^0(k) &= [\tau / (8da^2 \lambda_{ab}^2 k_z^2)] \ln(1 + a^2 k_z^2 / 4\pi) \end{aligned} \quad (2)$$

where $\tau = \phi_0^2 d / (4\pi^2 \lambda_{ab}^2)$ sets the energy scale and λ_{ab} is the magnetic penetration length parallel to the layers; $\tau \approx 10^3 - 10^4 K$ for YBCO or BSCCO parameters¹. Note the strong dispersion of $c_{44}^0(k)$ so that $c_{44}^0(k)$ decreases by the large factor $(d/a)^2$ when k varies from $k \lesssim 1/a$ to $1/a \lesssim k < \pi/d$.

The Josephson phase between the layers n and $n+1$ at position \mathbf{r} in both layers involves contributions from a nonsingular component and from singular vortex terms. The singular phase around a pancake vortex at position

$\mathbf{R}_l + \mathbf{u}_l^n$ is $\alpha(\mathbf{r} - \mathbf{R}_l - \mathbf{u}_l^n)$ where $\alpha(\mathbf{r}) = \arctan(y/x)$ with $\mathbf{r} = (x, y)$. We assume that all vortices belong to the flux lines, i.e. there are no free vacancies or interstitials.

The Josephson phase involves the interlayer phase difference from the pancake singularities $\alpha(\mathbf{r} - \mathbf{R}_l - \mathbf{u}_l^n) - \alpha(\mathbf{r} - \mathbf{R}_l - \mathbf{u}_l^{n+1})$, which after expansion in \mathbf{u}_l^n becomes (Eq. 19 of the companion article³⁷)

$$b_n(\mathbf{r}) = 2\pi i d \int_{BZ} \frac{d^2 \mathbf{q} dk}{(2\pi)^3} e^{-i\mathbf{q} \cdot \mathbf{r} - iknd} (e^{ikd} - 1) \frac{u^{tr}(\mathbf{q}, k)}{\mathbf{q}}. \quad (3)$$

We consider first a simplified model which neglects the nonsingular part of the Josephson phase. The nonsingular phase is essential for evaluating displacement fluctuations (section IV), however for the purpose of the phase transitions under study it can be neglected (justified by Appendices A,B). We have then an effective Hamiltonian for wavevectors $|q| < Q_0$, (Eq. (23) of the companion article³⁷)

$$\mathcal{H}_{pure}^{(1)}/T = \frac{1}{2} \sum_{\mathbf{q}, k} c(q, k) q^2 |b(\mathbf{q}, k)|^2 - \frac{E_J}{T} \sum_n \int d^2 \mathbf{r} \cos b_n(\mathbf{r}) \quad (4)$$

where E_J is the interlayer Josephson coupling energy per unit area and

$$c(q, k) = \frac{a^4}{(2\pi d)^2 T} [c_{44}^0(k) + \frac{q^2}{k_z^2} c_{66}^0] \equiv c(k) + c' \frac{q^2}{k_z^2} \quad (5)$$

The last equality defines $c(k)$ and c' , i.e.

$$\begin{aligned} c(k) &= \frac{\tau a^2}{32\pi^2 T d^3 \lambda_{ab}^2} \frac{\ln(1 + a^2 k_z^2 / 4\pi)}{k_z^2} \\ c' &= \frac{\tau a^2}{64\pi^2 T d^3}. \end{aligned} \quad (6)$$

Since $\nabla \alpha \sim 1/r$ decays slowly, even if \mathbf{u}_l^n are small the contribution of many vortices which move in phase ($q \rightarrow 0$) leads to a divergent response of $b_n(\mathbf{r})$, i.e the $1/q$ factor in Eq. (3). This leads to a decoupling transition^{30,37,38}, which at weak E_J is (Eqs. (27, 40) of the companion article³⁷)

$$T_d^0 = \frac{4a^4}{d^2} \left(\int \frac{dk}{c_{44}^0(k)} \right)^{-1} \approx \frac{\tau a^2 \log(a/d)}{4\pi \lambda_{ab}^2}. \quad (7)$$

We note that melting and related dislocations have been neglected. An estimate of T_m by the Lindemann criterion yields^{20,42} $T_m \approx \tau$, hence our description near T_d^0 is limited to $a \lesssim \lambda_{ab}$.

We proceed now to study the disorder term. A second assumption of the simplified version is that of linearized disorder, i.e. small fluctuations $|\mathbf{u}_l^n| \ll a$. Consider a short range pinning potential $U_{pin}^n(\mathbf{r})$ with the coupling

$$\mathcal{H}_{pin} = \int d^2 r \sum_{n,l} U_{pin}^n(\mathbf{r}) p(\mathbf{r} - \mathbf{R}_l - \mathbf{u}_l^n) \quad (8)$$

where $p(\mathbf{r})$ is a shape function for a vortex of size ξ_0 and the disorder has short range correlation

$$\langle U_{pin}^n(\mathbf{r}) U_{pin}^{n'}(\mathbf{r}') \rangle = \frac{1}{2} \bar{U} \delta_{n,n'} \delta(\mathbf{r} - \mathbf{r}') \quad (9)$$

Expanding Eq. (8) to first order in \mathbf{u}_l^n and averaging $U_{pin}^n(\mathbf{r})$ by the replica method^{22,45} leads to a disorder term in the free energy

$$\mathcal{H}_{dis}^{(1)}/T = \frac{\bar{U} \bar{p}}{4T^2} \sum_{n,l} \sum_{\alpha, \beta} \mathbf{u}_l^{n,\alpha} \cdot \mathbf{u}_l^{n,\beta} \quad (10)$$

where α, β are replica indices. The average involves

$$\int \partial_i p(\mathbf{r}) \partial_j p(\mathbf{r}) d^2 r = \bar{p} \delta_{ij} \quad (11)$$

with \bar{p} of order 1.

The replicated Hamiltonian of the simplified version, keeping only transverse displacements, is therefore

$$\begin{aligned} \mathcal{H}^{(1)}/T = & \frac{1}{2} \sum_{\mathbf{q}, k; \alpha, \beta} [c(q, k) q^2 \delta_{\alpha, \beta} - s_0 \frac{q^2}{k_z^2}] b^\alpha(\mathbf{q}, k) b^{\beta*}(\mathbf{q}, k) \\ & - \frac{E_J}{T} \sum_{n; \alpha} \int d^2 r \cos b_n^\alpha(\mathbf{r}) - \frac{E_v}{T} \sum_{n; \alpha \neq \beta} \int d^2 r \cos[b_n^\alpha(\mathbf{r}) - b_n^\beta(\mathbf{r})] \end{aligned} \quad (12)$$

where

$$s_0 = \frac{\bar{U} \bar{p}}{2T^2} \frac{a^2 d}{(2\pi d^2)^2}. \quad (13)$$

It is found useful below to define a dimensionless disorder parameter s ,

$$s = \frac{8\pi \bar{U} \bar{p} \lambda_{ab}^4}{\tau^2 a^2 \ln^2(a/d)}. \quad (14)$$

The inter-replica Josephson coupling, i.e. the E_v term in Eq. (12), is generated from the E_J term in second order renormalization group (RG). It is essential to keep the E_v term from the start since it couples different replica indices and leads to distinct physics by RSB, as shown below.

We note that a similar two-dimensional (2D) model has been studied by RSB and RG methods^{43,44}. As shown in the next section, finite values of k dominate the phase transitions, so that a certain k averages of the coefficients in Eq. (12) lead to a 2D problem with the same q singularities as in (12). Indeed the RSB solution below has the same structure as the 2D case⁴³ with a temperature parameter $t = T/T_d^0$ and a disorder parameter s (Eq. 14). In view of this similarity, it is useful to quote the RG equations of the 2D model⁴³ in terms of $u = \xi^2 E_J$ and $v = \xi^2 E_v$,

$$\begin{aligned} du &= [2u(1-t-s) - 2\gamma' uvt] d \ln \xi \\ dv &= [2v(1-2t) + \frac{1}{2}\gamma' s u^2 - 2\gamma' t v^2] d \ln \xi \\ dt &= -2\gamma''^2(t+s)t^2 u^2 d \ln \xi \\ d(s/t^2) &= 16\gamma''^2 t v^2 d \ln \xi \end{aligned} \quad (15)$$

where the initial value of the scale ξ is a and γ', γ'' are numbers of order 1. As expected, E_v is generated by sE_J^2 .

The full model involves a nonsingular phase $\theta_n(\mathbf{r})$ in addition to the pancake fluctuations via $b_n(\mathbf{r})$. The Hamiltonian of the pure system is then (Eq. 21 of the companion article³⁷)

$$\begin{aligned} \mathcal{H}_{pure}\{b, \theta\}/T = & \frac{1}{2} \sum_{q, k} G_f^{-1}(\mathbf{q}, k) |\theta(\mathbf{q}, k)|^2 + \frac{1}{2} \sum_{\mathbf{q}, k} c(\mathbf{q}, k) q^2 |b(\mathbf{q}, k)|^2 \\ & - \frac{E_J}{T} \sum_n \int d^2 r \cos[\theta_n(\mathbf{r}) + b_n(\mathbf{r})] \end{aligned} \quad (16)$$

where

$$G_f(q, k) = \frac{4\pi d^3 T}{\tau q^2} (\lambda_{ab}^{-2} + k_z^2). \quad (17)$$

Consider next the general form of the disorder coupling²⁰. Using the relation $\sum_l \delta^2(\boldsymbol{\rho} - \mathbf{R}_l) = \sum_l e^{i\mathbf{Q}_l \cdot \boldsymbol{\rho}}$ where \mathbf{Q}_l are reciprocal lattice vectors, the disorder coupling (8) becomes

$$\mathcal{H}_{pin} = - \int d^2 r \sum_n U_{pin}^n(\mathbf{r}) \int \frac{d^2 \rho}{a^2} p(r - \boldsymbol{\rho} - \mathbf{u}^n(\boldsymbol{\rho})) \sum_l e^{i\mathbf{Q}_l \cdot \boldsymbol{\rho}} \quad (18)$$

For $|\mathbf{Q}_l| < 1/\xi_0$ we can replace $p(\mathbf{r})$ by $\xi_0^2 \delta^2(\mathbf{r})$ so that

$$\mathcal{H}_{pin} = - \frac{\xi_0^2}{a^2} \int d^2 r \sum_n U_{pin}^n(\mathbf{r}) [1 + \boldsymbol{\nabla} \cdot \mathbf{u}^n(\mathbf{r})]^{-1} \sum_l e^{i\mathbf{Q}_l \cdot (\mathbf{r} - \mathbf{u}^n(\mathbf{r}))} \quad (19)$$

The coupling to long wavelength modes via $\nabla \mathbf{u}^n(\mathbf{r})$ is irrelevant²² in 3D so that the replica average of \mathcal{H}_{pin} becomes

$$\mathcal{H}_{dis}/T = \frac{g}{a^2} \sum_{\mathbf{Q}, \alpha, \beta, n} \int d^2r \cos[\mathbf{Q} \cdot (\mathbf{u}^{n, \alpha}(\mathbf{r}) - \mathbf{u}^{n, \beta}(\mathbf{r}))] \quad (20)$$

with $g = \bar{U} \xi_0^4 / T^2 a^2$. To relate this form to the linearized one (10) we expand in $\mathbf{u}^{n, \alpha}(\mathbf{r})$ and use $\sum_{\mathbf{Q}} \mathbf{Q}^2 \approx \frac{a^2}{4\pi} \int^{1/\xi_0^2} Q^2 dQ^2 \approx a^2 / 8\pi \xi_0^4$ so that (10) is obtained if $\bar{p} \approx 1/2\pi$. The coupling g can then be written as

$$g = \frac{\bar{U} \xi_0^4}{T^2 a^2} = s \frac{\tau^2 \xi_0^4 \ln^2(a/d)}{4T^2 \lambda_{ab}^4}. \quad (21)$$

We are interested here in BG effects on the $q \rightarrow 0$ singularity associated with the decoupling transition, i.e. the long range properties of the BG. The BG domain size is defined by the scale R where the displacement correlation starts to diverge as $\ln r$. It is reasonable to expect that this scale is determined by the shortest \mathbf{Q} , as indeed shown for a system with regular elasticity²², i.e. far from decoupling. We consider then the disorder term with just the (two) shortest reciprocal wavevectors $|\mathbf{Q}| \approx 2\pi/a$. The full Hamiltonian is then

$$\begin{aligned} \mathcal{H}/T = & \sum_{\alpha} \frac{1}{T} \mathcal{H}_{pure}\{b^{\alpha}, \theta^{\alpha}\} - \frac{E_v}{T} \sum_{n; \alpha \neq \beta} \int d^2r \cos[b_n^{\alpha}(\mathbf{r}) - b_n^{\beta}(\mathbf{r}) + \theta_n^{\alpha}(\mathbf{r}) - \theta_n^{\beta}(\mathbf{r})] \\ & - \frac{g}{a^2} \sum_{\alpha \neq \beta, n} \int d^2r \cos[\mathbf{Q} \cdot (\mathbf{u}^{n, \alpha}(\mathbf{r}) - \mathbf{u}^{n, \beta}(\mathbf{r}))]. \end{aligned} \quad (22)$$

III. PHASE DIAGRAM

In this section we consider the simplified version, Eq. (12). This assumes that displacements are within finite domains and Bragg glass effects are neglected; also the nonsingular phase is neglected here. Appendices A and B show that these assumptions are justified for the purpose of our phase diagram. The nonsingular phase is essential for evaluating displacement fluctuations, as studied in Appendix C.

The RSB method⁴⁵ proceeds by employing a variational free energy $\mathcal{F}_{var} = \mathcal{F}_0 + \langle \mathcal{H} - \mathcal{H}_0 \rangle$ with \mathcal{F}_0 the free energy corresponding to

$$\mathcal{H}_0 = \frac{1}{2} \sum_{\mathbf{q}, k; \alpha, \beta} G_{\alpha, \beta}^{-1}(\mathbf{q}, k) b^{\alpha}(\mathbf{q}, k) b^{\beta*}(\mathbf{q}, k) \quad (23)$$

and $G_{\alpha, \beta}(\mathbf{q}, k)$ is determined by an extremum condition on \mathcal{F}_{var} . We define the following averages $\langle \dots \rangle_0$ with respect to H_0 ,

$$\begin{aligned} \langle \cos b_n^{\alpha}(\mathbf{r}) \rangle_0 &= e^{-\frac{1}{2} A_{\alpha}} \\ A_{\alpha} &= \sum_{\mathbf{q}, k} G_{\alpha, \alpha}(q, k) \end{aligned} \quad (24)$$

$$\begin{aligned} \langle \cos[b_n^{\alpha}(\mathbf{r}) - b_n^{\beta}(\mathbf{r})] \rangle_0 &= e^{-\frac{1}{2} B_{\alpha, \beta}} \\ B_{\alpha, \beta} &= 2 \sum_{\mathbf{q}, k} [G_{\alpha, \alpha}(\mathbf{q}, k) - G_{\alpha, \beta}(\mathbf{q}, k)] \end{aligned} \quad (25)$$

so that

$$\begin{aligned} \mathcal{F}_{var}/T = & \frac{1}{2} \sum_{\mathbf{q}, k} Tr[\ln G(q, k) + (G^{-1}(q, k) - c(q, k) q^2 \hat{I} - s_0 \frac{q^2}{k_z^2} \hat{L}) G(q, k)] \\ & - \frac{E_J}{T} \sum_{\alpha} e^{-\frac{1}{2} A_{\alpha}} - \frac{E_v}{T} \sum_{\alpha \neq \beta} e^{-\frac{1}{2} B_{\alpha, \beta}} \end{aligned} \quad (26)$$

where $\hat{I}_{\alpha, \beta} = \delta_{\alpha, \beta}$ and $\hat{L}_{\alpha, \beta} = 1$.

The variational equation $\delta F_{var}/\delta G_{\alpha,\beta} = 0$ yields

$$G_{\alpha,\beta}^{-1}(q, k) = [c(q, k)q^2 + z]\delta_{\alpha,\beta} - s_0(q^2/k_z^2) - \sigma_{\alpha,\beta} \quad (27)$$

$$z = \frac{E_J}{Td} e^{-\frac{1}{2}A_\alpha} \quad (28)$$

$$\sigma_{\alpha,\beta} = \frac{E_v}{Td} [e^{-\frac{1}{2}B_{\alpha,\beta}} - \delta_{\alpha,\beta} \sum_{\gamma} e^{-\frac{1}{2}B_{\alpha,\gamma}}] \quad (29)$$

where z is a renormalized Josephson coupling. In the replica limit with the number of replicas $n \rightarrow 0$ the RSB⁴⁵ method represents each matrix as a hierarchy of matrices, e.g. $\sigma_{\alpha,\beta}$ is represented by $\sigma(u)$, with $0 < u < 1$ and a diagonal component $\tilde{\sigma}$. We parameterize therefore $G_{\alpha,\beta}^{-1}$ by \tilde{a} and $a(u)$, where

$$\begin{aligned} \tilde{a} &= c(q, k)q^2 - s_0 \frac{q^2}{k_z^2} + z - \tilde{\sigma} \\ a(u) &= -s_0 \frac{q^2}{k_z^2} - \sigma(u). \end{aligned} \quad (30)$$

The amount by which the replica symmetry is broken is measured by a glass order parameter

$$\Delta(u) = u\sigma(u) - \int_0^u \sigma(v) dv. \quad (31)$$

The inverse matrix $G_{\alpha,\beta}$ is represented by \tilde{b} and $b(u)$, where⁴⁵ (see also Appendix B of Ref. 43)

$$\begin{aligned} \tilde{b} &= \frac{1}{\tilde{a} - \langle a \rangle} \left[\frac{-a(0)}{\tilde{a} - \langle a \rangle} + 1 + \int_0^1 \frac{dv}{v^2} \frac{\Delta(v)}{\tilde{a} - \langle a \rangle + \Delta(v)} \right] \\ \tilde{b} - \langle b \rangle &= \frac{1}{u[\tilde{a} - \langle a \rangle + \Delta(u)]} - \int_u^1 \frac{dv}{v^2} \frac{1}{\tilde{a} - \langle a \rangle + \Delta(v)} \end{aligned} \quad (32)$$

and

$$\begin{aligned} \langle a \rangle &= \int_0^1 a(v) dv = s_0 \frac{q^2}{k_z^2} - \langle \sigma \rangle \\ \tilde{a} - \langle a \rangle + \Delta(u) &= c(q, k)q^2 + z + \Delta(u). \end{aligned} \quad (33)$$

$B(u)$ can be written, using (25) and the inversion formula (32), as

$$\frac{1}{2}B(u) = \frac{g(u)}{u} - \int_u^1 \frac{g(v)}{v^2} \quad (34)$$

where

$$g(u) = \sum_{\mathbf{q}, k} \frac{1}{c(k)q^2 + z + \Delta(u)} = \int \frac{dk}{2\pi} \frac{1}{4\pi c(k)} \left[\ln \frac{\Delta_c}{z + \Delta(u)} \right] + C_1. \quad (35)$$

and

$$C_1 = \int \frac{dk}{8\pi^2 c(k)} \ln \frac{c(k)}{c(\pi/d)}. \quad (36)$$

Here $c(q, k)$ of Eq. (5) is replaced by $c(k)$ as defined in (5, 6) while the q^2 term in Eq. (5) amounts to redefining the upper cutoff into $q_u^2 = 4 \ln(a/d)/\lambda_{ab}^2$, (considering $k \approx \pi/d$ as the dominant range of the following k integration) and $\Delta_c = c(\pi/d)q_u^2$. In the following a variable t is temperature in units T_d^0 of the pure system (Eq. 7), i.e.

$$t = \frac{T}{T_d^0} = \int \frac{dk}{16\pi^2} \frac{1}{c(k)}. \quad (37)$$

Eq. (35) is then

$$g(u) = 2t \ln \frac{\Delta_c}{z + \Delta(u)} + C_1. \quad (38)$$

To find $\Delta(u)$ we note that Eq. (29) is equivalent to $\sigma(u) = (E_v/Td) \exp[-B(u)/2]$. Differentiating this equation and using $\Delta'(u) = -u\sigma'(u)$ we obtain

$$\frac{\Delta'(u)}{u} = -\frac{d}{du} \left[\frac{\Delta'(u)}{g'(u)} \right], \quad (39)$$

which by using (38) can be written as

$$\left(\frac{1}{u} - \frac{1}{2t} \right) \frac{d\Delta}{du} = 0. \quad (40)$$

The solution of this equation is a one step function, i.e. $\Delta(u)$ jumps at $u = 2t$ from zero to a constant value Δ_0 at $2t < u < 1$. The solution is therefore nontrivial if $t < 1/2$.

To complete the solution, the function $B(u)$ from (34) is needed

$$\begin{aligned} \frac{1}{2}B(u) &= C_1 + \ln \frac{\Delta_c}{z} + (2t-1) \ln \frac{\Delta_c}{z + \Delta_0} & u < 2t \\ &= C_1 + 2t \ln \frac{\Delta_c}{z + \Delta_0} & 2t < u < 1 \end{aligned} \quad (41)$$

which yields for $\sigma(u)$

$$\begin{aligned} \sigma(u) = \sigma_0 &= \frac{z}{z + \Delta_0} \sigma_1 & u < 2t \\ \sigma_1 &= \frac{E_v}{Td} \left(\frac{z + \Delta_0}{\Delta_c} \right)^{2t} e^{-C_1} & 2t < u < 1. \end{aligned} \quad (42)$$

Finally, from Eq. (31) we have $z + \Delta_0 = 2t\sigma_1$, hence,

$$\frac{z + \Delta_0}{\Delta_c} = \left(\frac{2E_v}{dT_d \Delta_c} e^{-C_1} \right)^{\frac{1}{1-2t}} \quad (43)$$

A consistent weak coupling solution is indeed possible only at $t < \frac{1}{2}$.

To find a second equation for z from (28) we need the first inversion formula in (32)

$$\tilde{G}(q, k) = \frac{\frac{s_0}{k_z^2 c(k)} + \frac{1}{2t}}{c(k)q^2 + z} + \frac{\sigma_0 - \frac{s_0 z}{k_z^2 c(k)}}{(c(k)q^2 + z)^2} + \frac{1 - \frac{1}{2t}}{c(k)q^2 + z + \Delta_0} \quad (44)$$

and after the \mathbf{q} summation

$$A_\alpha = \sum_{\mathbf{q}, k} \tilde{G}(q, k) = \int \frac{dk}{8\pi^2} \left[\frac{1}{2tc(k)} \ln \frac{z + \Delta_0}{z} + \frac{1}{c(k)} \ln \frac{\Delta_c}{z + \Delta_0} + \frac{\sigma_0}{zc(k)} \right] + C_1 + \frac{s_0}{8\pi^2} [I(z) + zI'(z)] \quad (45)$$

where

$$I(z) = \int \frac{dq^2 dk}{k_z^2 c(k)} \frac{1}{c(k)q^2 + z} \quad (46)$$

and $I'(z) = dI(z)/dz$. For $\Delta_0 \neq 0$ we have from Eq. (42) $\sigma_0 = z/2t$ while for $\Delta_0 = 0$ (possible at $t > \frac{1}{2}$ as found below) we have $\sigma_0 \sim z^{2t} \ll z$, hence, with s defined in (14),

$$A_\alpha = \ln(2etE_v/zd) + (s_0/8\pi^2) [I(z) + zI'(z)] \quad \Delta_0 \neq 0 \quad (47)$$

$$= C_1 + 2(t+s) \ln \frac{\Delta_c}{z} + 2s \quad \Delta_0 = 0. \quad (48)$$

Formally $I(z)$ diverges at $k = 0$; this divergence can be traced back to our assumption that the $\cos[\mathbf{Q} \cdot (\mathbf{u}_l^{n,\alpha} - \mathbf{u}_l^{n,\beta})]$ term is expanded into the s_0 term in Eq. (12). Retaining this cosine leads to domains of correlated \mathbf{u}_l^n . In Appendix

A the joint BG-JG solution is found and is shown to remove the $k \rightarrow 0$ divergence. A combined BG with non-singular phase solution is also shown in Appendix B to remove this divergence. The presence of BG, however, produces a term $\sim \ln^2 z$ in a regime near decoupling. This "anharmonic" regime is studied further in section IV. Excluding this anharmonic regime, the dominant part of $I(z)$ is

$$I_0(z) = 2 \int_{1/a}^{\pi/d} \frac{dk}{k_z^2 c(k)} \int \frac{dq^2}{c(k)q^2 + z} = \frac{\pi d}{4c^2(\pi/d)} \ln \frac{\Delta_c}{z} \quad (49)$$

The $I(z)$ term in Eq. (45) can then be written as

$$\frac{s_0}{8\pi^2} I(z) \approx \frac{s_0}{8\pi^2} I_0(z) = 2s \ln \frac{\Delta_c}{z}. \quad (50)$$

Therefore, the renormalized Josephson coupling of Eq. (28) is for $\Delta_0 \neq 0$, using Eq. (47),

$$\frac{z}{\Delta_c} = e^{-1} \left(\frac{E_J^2}{2TtdE_v\Delta_c} \right)^{\frac{1}{1-2s}}. \quad (51)$$

Note that E_v is generated from E_J by RG^{43,44}, i.e. $E_v \sim E_J^2$ initially; however, E_v is RG relevant at $t < \frac{1}{2}$ even in 1st order RG (Eq. 15), hence we consider E_v and E_J as comparable so that $E_J^2/(2TtdE_v\Delta_c) \ll 1$. Hence a consistent weak coupling $z/\Delta_c \ll 1$ solution is possible only for $s < \frac{1}{2}$. Thus $s = \frac{1}{2}$ marks a disorder induced decoupling with $z = 0$ at $s > \frac{1}{2}$.

Comparing Eqs. (43,51) shows that Δ_0 vanishes at $s = t$ (up to $O[\ln(E_J/E_v)/\ln E_v]$ term, small for $E_J \approx E_v \ll d\Delta_c T_d$). Formally there is a solution with $\Delta_0 < 0$ when $s < t$. However, the average distribution⁴⁵ of $|b(\mathbf{q}, k)|^2$, which is $\sim \exp[-|b(\mathbf{q}, k)|^2/G_{\alpha,\alpha}(\mathbf{q}, k)]$, is acceptable only if $G_{\alpha,\alpha}(\mathbf{q}, k) > 0$; this is therefore a thermodynamic stability criterion. Note in particular from Eq. (44)

$$G_{\alpha\alpha}(q=0, k) = \frac{1}{2t} \left(\frac{2}{z} - \frac{1-2t}{z+\Delta_0} \right). \quad (52)$$

When $s < t$ and $\Delta_0 < 0$ the power dependence in Eq. (43) implies that $z + \Delta_0 \ll z$ (unless too close to $t = s$, i.e. $s - t \sim 1/|\ln E_v|$) and therefore $G_{\alpha\alpha}(q=0, k) < 0$. This shows that only $\Delta_0 > 0$ is acceptable.

Thus the regime where both z, Δ_0 are finite is limited to $s < \frac{1}{2}, t < s$; we term this regime the coupled Josephson Glass (JG) phase. The "coupled" notation means that the renormalized Josephson coupling is finite, i.e. $z \neq 0$. The glass parameter vanishes (continuously) at $t = s$ while the Josephson coupling vanishes (with an apparent discontinuity - see section IV) at $s = \frac{1}{2}$ (see Fig. 1). For $s > \frac{1}{2}$ and $t < \frac{1}{2}$ the solution is $z = 0$ while $\Delta_0 \neq 0$ satisfies Eq. (43), i.e. it is a *decoupled* JG phase. Recall that the JG order parameter Δ_0 is due to E_v which is initially generated by E_J . In fact, RG shows (see a similar effect in Fig. 3 of the companion article³⁷ for the pure system) that E_J first increases (scaling from ξ_0 to $1/q_u$), generating the E_v term, and only at scales beyond $1/q_u$ E_J decreases to zero. It is remarkable then that E_J is renormalized to zero while the JG order survives, much like the smile of the Cheshire cat.

Finally, for $\Delta_0 = 0$ a replica symmetric solution is valid at $s < t$, which upon using Eqs. (28, 48) becomes

$$\frac{z}{\Delta_c} = \left(\frac{E_J}{Td\Delta_c} e^{-s-\frac{1}{2}C_1} \right)^{\frac{1}{1-s-t}}. \quad (53)$$

Thus $s + t = 1$ for $s < \frac{1}{2}$ defines a "thermal" decoupling transition.

The interpretation of the phase diagram needs to be supplemented by a few observations from an RG analysis. The RSB results above coincide with those of a 2D model where the parameters t, s of the 3d system, as suitable k averages (Eqs. 37,14), correspond to Hamiltonian parameters of the 2D system⁴³. With this correspondence in mind, we infer next some qualitative modifications by using the 2D RG equations^{43,44}, Eq. (15). Note first that in a coupled phase z is RG relevant and therefore E_v , which is generated to order z^2 , is relevant too, hence a weak glass phase is expected also in the regime $s < t < 1 - s$; this weak glass order is not captured by the RSB solution. The line $t = s$ for $s < \frac{1}{2}$ is therefore not a strict phase transition but rather a crossover line. RG suggests this crossover line at $t = \frac{1}{2}$: at $t < \frac{1}{2}$ RG yields E_v which is largely independent of z , hence a strong JG order, while at $t > \frac{1}{2}$ RG generates $E_v \sim z^2$ with a weak JG order. The stability of the RSB solution shows that in fact the crossover line is at $t = s$.

The RG, shows also a disordered induced decoupling, since Eq. (15) has a fixed point with $u^* = 0$ and $v^* = (1 - 2t)/\gamma t$, stable at $t < \frac{1}{2}$ and strong disorder. Note that for this solution $s \sim \ln \xi$ increases with scale ξ , hence the correlator $\Gamma(r) = \langle \cos b_n^\alpha(\mathbf{r}) \cos b_n^\alpha(0) \rangle$ which by RSB decays as r^{-2-4s} is actually decaying faster as $\ln \Gamma(r) \sim -\ln^2 r$. Explicit solution of the 2D RG equations⁴⁴ found indeed a phase diagram very similar to that in Ref. 43 or in Fig. 1.

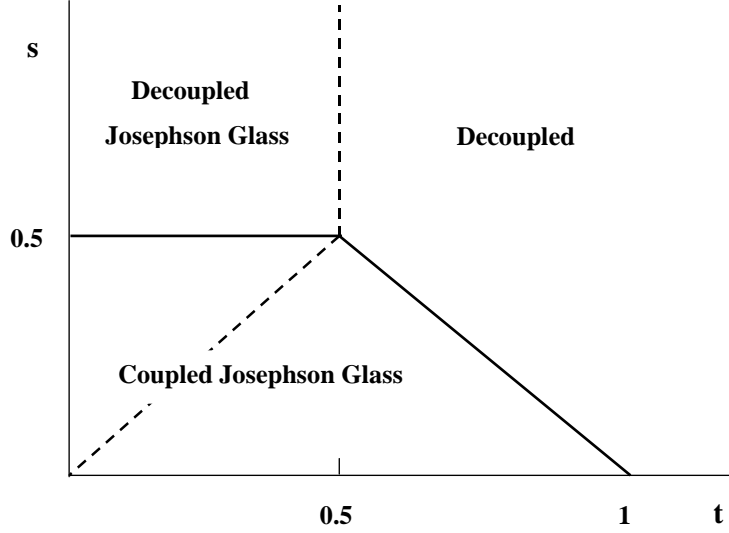


FIG. 1: Phase diagram. Full lines are decoupling lines where the Josephson coupling vanishes. The upper dashed line is a depinning transition where the Josephson glass parameter vanishes; the lower dashed line is a crossover into a weaker JG phase or weaker pinning.

The phase diagram, shown in Fig. 1, has three phase transition lines and one crossover line which all meet at a multicritical point $s = t = 1/2$. The dashed line within the coupled JG phase is the crossover line. We interpret the transition where Δ_0 vanishes as a depinning transition, i.e. the JG order parameter provides an additional pinning to that from the Bragg glass. The phase diagram has then a decoupling line which crosses a depinning line at the multicritical point. The decoupling line has a disorder driven section, $s = \frac{1}{2}$ at $t < \frac{1}{2}$.

The phase diagram in terms of field and temperature is derived by defining B_0, T_0 as the field and temperature value of the multicritical point and is shown in Fig. 2. B_0 is determined by the disorder strength via $s = \frac{1}{2}$ while $T_0 = \frac{1}{2}T_d(a = \sqrt{B_0/\phi_0})$ (Eq. 7). Hence $s = B/2B_0$ and $t = TB/T_0B_0$, up to $\ln B$ terms. Since s increases with B the $s = \frac{1}{2}$ line defines a decoupling transition from a coupled JG phase at low B to a decoupled JG phase at high fields.

The coupled JG phase at $B < B_0$ undergoes a crossover transition at $t = s$, i.e. at $T = T_0$ (up to $\ln B$ factors). Therefore at $T > T_0$ the glass parameter Δ_0 is significantly reduced implying a depinning crossover from strong to weak pinning. The decoupled JG phase undergoes a depinning transition into a decoupled phase at $T = B_0T_0/B$. Note that all phases, even the high T decoupled one, are Bragg glass phases of the flux lattice; in the decoupled phase the lattice is maintained by the interlayer electromagnetic coupling.

The JG coupled phase at $T > T_0$ undergoes a decoupling transition at $t = 1 - s$, i.e. $B = 2B_0T_0/(T + T_0)$. This transition is continuous; the variational method of the pure system has been formally extended to higher J/T and found to be of first order³⁰. As shown in the companion article I, the transition remains 2nd order when proper 2nd order RG is employed. Disorder, however, leads to an apparent discontinuity near decoupling, as discussed in the next section.

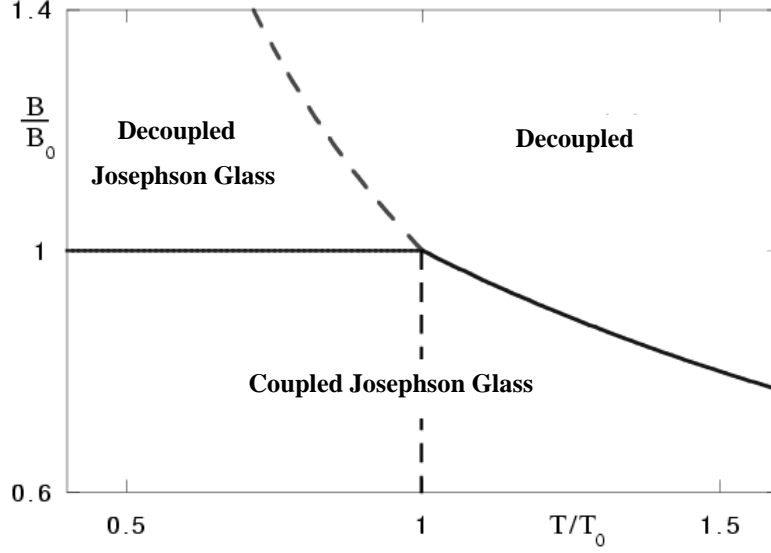


FIG. 2: Phase diagram in terms of field and temperature. Full lines are decoupling lines [$B = B_0$ and $B = 2B_0T_0/(T + T_0)$] where the Josephson coupling vanishes. The upper dashed line is a depinning transition ($T = B_0T_0/B$) where the Josephson glass parameter vanishes; the lower dashed line ($T = T_0$) is a crossover into weaker pinning.

IV. DOMAIN SIZES

In this section we estimate various domain sizes and evaluate displacement fluctuations which identify these sizes. Remarkably, the expressions for the domain sizes are confirmed (up to numerical prefactors) by BG solutions (Appendices A-C). The nonsingular phase, which was irrelevant for the purpose of the phase diagram in section III, is essential now.

To appreciate the effect of the nonsingular phase θ , we briefly review the derivation of the transverse tilt modulus c_{44} of a pure flux lattice⁴². The Josephson phase involves the contribution of pancake fluctuations via $b_n(\mathbf{r})$ as well as a nonsingular phase, with the Hamiltonian Eq. (16). To identify c_{44} we expand the Josephson coupling to 2nd order in $\tilde{b}(\mathbf{q}, k) = b(\mathbf{q}, k) + \theta(\mathbf{q}, k)$,

$$\begin{aligned} \mathcal{H}_{pure}/T = & \frac{1}{2} \sum_{q,k} \left\{ \left[G_f^{-1}(q, k) + \frac{E_J}{Td} \right] \left| \tilde{b}(\mathbf{q}, k) - b(\mathbf{q}, k) \frac{G_f^{-1}(q, k)}{G_f^{-1}(q, k) + \frac{E_J}{Td}} \right|^2 + \right. \\ & \left. \frac{G_f^{-1}(q, k) \frac{E_J}{Td}}{G_f^{-1}(\mathbf{q}, k) + \frac{E_J}{Td}} |b(\mathbf{q}, k)|^2 + \frac{1}{2} c(q, k) |b(\mathbf{q}, k)|^2 + O(\tilde{b}^4(\mathbf{q}, k)) \right\}. \end{aligned} \quad (54)$$

The first term decouples from $b(\mathbf{q}, k)$ and with $|b(\mathbf{q}, k)|^2 = (2\pi d^2)^2 k_z^2 |u^{tr}(q, k)|^2 / q^2$ (Eq. 3) we identify^{40,41,42}

$$c_{44}(q, k) = c_{44}^0(k) + \frac{B^2}{4\pi} \frac{1}{1 + \lambda_c^2 q^2 + \lambda_{ab}^2 k^2} + \frac{2B\phi_0}{(8\pi\lambda_c)^2} \ln(a^2/4\pi\xi_0^2) \quad (55)$$

where $\lambda_c^2 = \lambda_{ab}^2 \tau / (4\pi d^2 E_J)$; the last term is from reducing high momenta of the 2nd term of (54) into the 1st Brillouin zone.

The second term of $c_{44}(q, k)$ is peculiar: at $q \neq 0$ it vanishes when E_J vanishes and $\lambda_c \rightarrow \infty$, as it should. However, at $q = 0$ this term seems to survive even if $\lambda_c \rightarrow \infty$. The origin of this peculiarity is that the harmonic expansion of the Josephson cosine term which identifies c_{44} fails⁴² when both $q, 1/\lambda_c \rightarrow 0$. The shift in the 1st term of Eq. (54) identifies an expansion parameter⁴² with terms $\sim q^2 k_z^2 |u_T(\mathbf{q}, k)|^2 / [q^2 + \lambda_c^{-2} (1 + \lambda_{ab}^2 k_z^2)]^2$, which diverge when both $q, 1/\lambda_c \rightarrow 0$ and the expansion becomes invalid. In fact, the nonlinear cosine term replaces E_J/Td by z or λ_c is

replaced by a renormalized

$$\lambda_c^R = \sqrt{\lambda_{ab}^2 \tau / (4\pi T d^3 z)} \quad (56)$$

which diverges at decoupling. Hence usual elasticity at $q, 1/\lambda_c^R \rightarrow 0$ near decoupling is ill defined.

The Bragg glass domain size R_{BG} (parallel to the layers) sets a scale for the relevant q values. When $R_{BG} > \lambda_c^R$ the tilt modulus is large, containing the $B^2/4\pi$ term of Eq. (55). However, as decoupling at the field B_0 is approached λ_c^R diverges so that when $R_{BG} < \lambda_c^R$ Eq. (55) fails to describe c_{44} on the scale of $q \approx 1/R_{BG}$. This defines an anharmonic crossover regime where usual elasticity cannot be used to derive Bragg glass properties. Finally, at $B > B_0$ elasticity is restored and c_{44} is reduced to the first term in Eq. (55). The main interest is in the regime of strong fields, i.e. $a \lesssim 2\lambda_{ab}$ where $T_0 \ll \tau$ is below melting. Thus at $B < B_0$ and for sufficiently large domains the second term in Eq. (55) dominates and c_{44} has an apparent discontinuity,

$$c_{44} = c_{44}^+ = \pi \lambda_{ab}^2 \tau / da^4 \quad \lambda_c^R < R_{BG} \quad (57)$$

$$= c_{44}^- = \tau / (32\pi \lambda_{ab}^2 d) \quad \lambda_c^R = \infty \quad (58)$$

Hence c_{44} is reduced within the anharmonic regime by the small factor

$$\epsilon = a^4 / (32\pi^2 \lambda_{ab}^4). \quad (59)$$

The apparent discontinuity in c_{44} affects also the domain sizes which can be estimated by a dimensional argument^{21,22}. Consider the tilt c_{44} and shear c_{66} terms of the elasticity Hamiltonian for the displacement $\mathbf{u}(\mathbf{r})$ and its transverse component $\mathbf{u}_T(\mathbf{r})$. Rescaling parallel and perpendicular lengths yields an isotropic form^{20,23}, which together with the pinning energy (19) yield (ignoring elasticity of longitudinal displacements)

$$\mathcal{H} = \int d^3r \left\{ \frac{1}{2} c_{44}^{1/3} c_{66}^{2/3} [\nabla u_T(\mathbf{r})]^2 - (\xi_0^2 / a^2 d) U_{pin}(\mathbf{r}) \sum_{\mathbf{Q}} \cos \mathbf{Q} \cdot [\mathbf{r} - \mathbf{u}(\mathbf{r})] \right\} \quad (60)$$

where the disorder coupling to $\nabla u_T(\mathbf{r})$ is neglected. Disorder average over configurations $\mathbf{u}(\mathbf{r})$ and $\mathbf{u}'(\mathbf{r})$ yields $\sum_{\mathbf{Q}} \cos \mathbf{Q} \cdot [\mathbf{u}(\mathbf{r}) - \mathbf{u}'(\mathbf{r})]$; the sum is cutoff by $Q \lesssim \langle u_T^2 \rangle^{-1/2}$ where $\langle u^2 \rangle \approx \langle u_T^2 \rangle$ are the fluctuations in a domain of size R' . Within this cutoff the cosine can be expanded and summed so that averaging Eq. (60) yields

$$\langle H \rangle / R'^3 = \frac{1}{2} c_{44}^{1/3} c_{66}^{2/3} \langle u_T^2 \rangle R'^{-2} - \bar{U}^{1/2} \xi_0^2 / [a^2 d \langle u_T^2 \rangle R'^3]^{1/2}. \quad (61)$$

Minimizing with respect to R' yields $R' \sim \langle u_T^2 \rangle^3$, i.e. the Flory exponent²². The domain size parallel to the layers is then (up to $\ln(a/d)$ and a numerical prefactor)

$$\begin{aligned} R^+ &\approx (\lambda_{ab}/a)^5 \langle u_T^2 \rangle^3 / (s \xi_0^4 d) & \lambda_c^R < R \\ R^- &\approx (\lambda_{ab}/a)^3 \langle u_T^2 \rangle^3 / (4\pi s \xi_0^4 d) & \lambda_c^R = \infty \end{aligned} \quad (62)$$

The pinning length $R = R_p$ is given by Eq. (62) with $\langle u_T^2 \rangle \approx \xi_0^2$. To allow for large pinning domains one needs either $a \ll \lambda_{ab}$ or to allow for domains with a somewhat larger fluctuations in $\langle u_T^2 \rangle$; the latter increases R_p very rapidly since it increases with the 6-th power of u_T . The critical current can now be estimated^{20,21} by balancing the Lorenz force $j_c B R^3 / c$ with the pinning force $\langle H \rangle / \xi_0$ (evaluated at the minimum of Eq. (61)), leading to $j_c \sim 1/c_{44}$. Increasing the field within the anharmonic regime decreases c_{44} by the factor ϵ so that j_c is enhanced by a $1/\epsilon$ factor which is significant when $a \lesssim \lambda_{ab}$.

A second length scale $R = R_{BG}$ is identified by Eq. (62) with the fluctuations $\langle u_T^2 \rangle \approx a^2$. The proper definition of R_{BG} is the scale for the onset of the $\ln r$ form for the displacement correlation function, as inferred in Eq. (A26) or (B8). It is remarkable that Eq. (62) gives the correct form for R_{BG} , up to a numerical prefactor, i.e. Eqs. (A26, B8). Eq. (62) shows that R_{BG} is reduced by $\epsilon^{1/2}$ through the anharmonic regime. The onset of the anharmonic regime is at $R_{BG}^+ \approx \lambda_c^R$, i.e.

$$\lambda_c^R \approx 10^{-3} \frac{a \lambda_{ab}^5}{s d \xi_0^2} \quad (63)$$

with a numerical prefactor from the BG solution (Eqs. A26, B8). For BSCCO or YBCO parameters at $s \approx \frac{1}{2}$ this reduces to $\lambda_c^R / \lambda_{ab} \approx 10^5$, i.e. the initial anisotropy of $\lambda_c / \lambda_{ab} = 10 - 100$ has to increase to $\approx 10^5$. Since z is exponentially renormalized (Eqs. 51, 53) this anharmonic range may be observable.

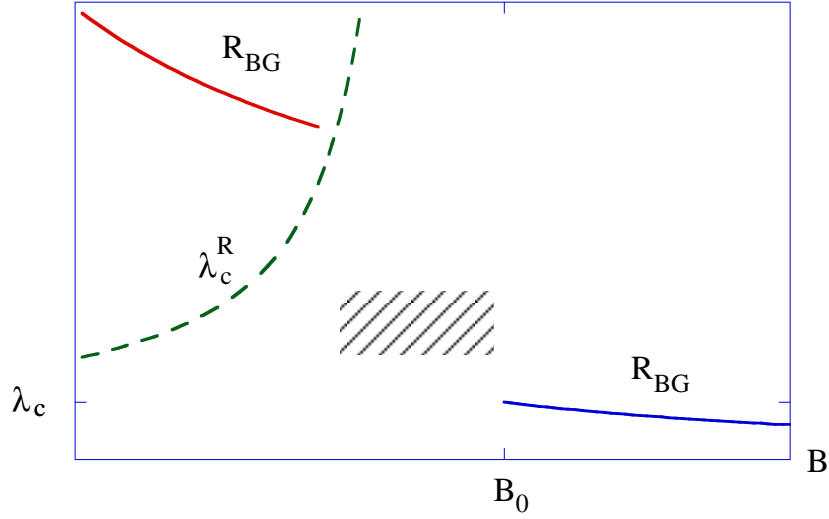


FIG. 3: Bragg glass domain size R_{BG} parallel to the layers and the renormalized London length perpendicular to the layers λ_c^R ; the latter diverges at the decoupling field B_0 . R_{BG} can be found from elasticity for $B < B_0$ only if $R_{BG} > \lambda_c^R$; otherwise, as in the hatched region, the elastic tilt modulus is ill defined.

Fig. 3 illustrates the lengths R_{BG} and λ_c^R , demonstrating the anharmonic regime within which R_{BG} has a significant drop and correspondingly j_c has an apparent jump. Note that even in the decoupled phase ($B > B_0$) R_{BG} is large for typical type II superconductors, $R_{BG} \approx \lambda_{ab}^3 a^3 / (4\pi s \xi_0^4 d) \gg a$, consistent with a decoupling transition within the Bragg glass phase, i.e. below a melting transition.

The solution of section III can also be extended to include the nonsingular phase. Since disorder is linearized, the pinning length R_p can be determined, though the BG length cannot. Appendix C develops this solution and shows that in the coupled phase R_p coincides with R^+ Eq. (62) (with $\langle u_T^2 \rangle \approx \xi_0^2$), up to a numerical prefactor.

The main result is then that the fluctuations in $u_T(r)$ behave with an effective c_{44} which is large when $q < 1/\lambda_c^R$ (Eq. (57)), i.e. for domain sizes $R_{BG} > \lambda_c^R$, while for $z = 0$ c_{44} is reduced (Eq. (58)). In the anharmonic region below decoupling (see Fig. 3) where $R_{BG} < \lambda_c^R$ a more complete form [e.g. Eq. (C8)] is required to interpolate between these limits. However, a method relying on an effective harmonic theory, such as RSB, is suspect within the anharmonic regime, since the system has no effective elastic constants. Furthermore, RSB signals this deficiency by producing a $\ln^2 z$ term, precisely in the the anharmonic regime found here, as shown in Appendices A and B.

V. PLASMA RESONANCE

Plasma resonance provides extremely useful data for identifying phases of vortex matter^{13,14,15,16}. In particular a jump in the resonance frequency ω_{pl} has shown^{15,16} that the Josephson coupling is strongly modified at the second peak transition. In this section we derive ω_{pl} in the ordered phases and also consider the fluctuation contribution in the disordered phase.

In presence of a weak time dependent electric field $E(t)$ in the direction perpendicular to the layers the Josephson relation imposes a time dependent addition $\delta\theta_n(t)$ to the Josephson phase. The kinetic energy has the form

$$E_K = \epsilon_0 \int \frac{E^2}{8\pi} d^3r = \frac{\epsilon_0 \hbar^2}{32\pi e^2 d} \sum_n \int d^2r \left(\frac{d\delta\theta_n(t)}{dt} \right)^2 \quad (64)$$

where ϵ_0 is a dielectric constant. Expanding the Josephson coupling $-E_J \sum_n \int d^2r \cos[b_n(\mathbf{r}) + \delta\theta_n(t)]$ yields to 2nd order $\frac{1}{2} E_J \langle \cos b \rangle [\delta\theta_n(t)]^2$, where $\langle \cos b \rangle$ implies a thermodynamic and spacial average on $\cos b_n(\mathbf{r})$ (The 1st order term has $\langle \sin b \rangle = 0$); more strictly one needs the averaged $\cos \tilde{b}_n(\mathbf{r})$. The plasma frequency is then

$$\omega_{pl}^2 = \frac{32\pi e^2 d}{\epsilon_0 \hbar^2} \langle \cos b \rangle. \quad (65)$$

The task is then to evaluate the thermodynamic average $\langle \cos b \rangle$.

Consider first the ordered phases where at least one of z and Δ_0 is finite. We start by evaluating \mathcal{F}_{var} of Eq. (26) for a general one step RSB, recover the solution of section III, and then identify $\langle \cos b \rangle$. The self mass term $\sigma_{\alpha,\beta}$ of Eq. (27) is written for a one step solution in the form

$$\hat{\sigma} = \sigma_0 \hat{L} + (\sigma_1 - \sigma_0) \hat{C} - [\sigma_0 n + (\sigma_1 - \sigma_0) m] \hat{I} \quad (66)$$

where $\hat{L}_{\alpha,\beta} = 1$ and \hat{C} has 1 elements in blocks of size $m \times m$ sitting consecutively along the diagonal, and 0 elements otherwise. For $n \rightarrow 0$ we identify $(\sigma_1 - \sigma_0)m = \Delta_0$ so that

$$\hat{G}(q, k) = [(c(q, k)q^2 + z + \Delta_0)\hat{I} + (-s_0 \frac{q^2}{k_z^2} - \sigma_0)\hat{L} - \frac{\Delta_0}{m}\hat{C}]^{-1} \equiv \alpha \hat{I} + \beta \hat{L} + \gamma \hat{C}. \quad (67)$$

It is straightforward to identify the coefficients of the inverse matrix

$$\begin{aligned} \alpha(q, k) &= \frac{1}{c(q, k)q^2 + z + \Delta_0}, & \alpha &= \sum_{\mathbf{q}, k} \alpha(q, k) = 2t \ln \frac{\Delta_c}{z + \Delta_0} + C_1 \\ \beta(q, k) &= \frac{s_0 \frac{q^2}{k_z^2} + \sigma_0}{[c(q, k)q^2 + z]^2}, & \beta &= \sum_{\mathbf{q}, k} \beta(q, k) = 2s(\ln \frac{\Delta_c}{z} - 1) + \frac{2t\sigma_0}{z} \\ \gamma(q, k) &= -\frac{1}{m}[\alpha(q, k) - \frac{1}{c(q, k)q^2 + z}], & \gamma &= \sum_{\mathbf{q}, k} \gamma(q, k) = \frac{2t}{m} \ln \frac{z + \Delta_0}{z} \end{aligned} \quad (68)$$

where the form of Eq. (50) is used for $I(z)$ in the 2nd line. The definition of $\hat{\sigma}$ identifies $\sigma_1 = 2E_v e^{-\alpha}/d$ and $\sigma_0 = 2E_v e^{-\alpha-\gamma}/d$. We follow a similar algebra in section IV of Ref. 43 to evaluate the free energy density per replica as

$$f(m, z, \Delta_0) = f_0 + (1 - \frac{1}{m}t\Delta_0 + (1 + \frac{s}{t})tz - \frac{E_v}{Td}(2t - m)e^{-\alpha-\gamma} + \frac{E_v}{Td}(1 - m)e^\alpha - \frac{E_J}{Td}e^{-\frac{1}{2}(\alpha+\beta+\gamma)} \quad (69)$$

where f_0 is m, z and Δ_0 independent. Minimizing $f(m, z, \Delta_0)$ yields $m = 2t$ and Eqs. (42,43,51) for $\sigma_0, \sigma_1, z + \Delta_0$ and z . A replica symmetric solution is also possible with $\Delta_0 = 0$ leading to Eq. (53). The free energy at minimum is

$$f_{min} = f_0 + (t - 1 + \frac{1}{4t})(\Delta_0 + z) + (s - \frac{1}{2})z. \quad (70)$$

The Hamiltonian Eq. (12) shows that $\langle \cos b \rangle = -Td(\partial f / \partial E_J)$. As discussed below Eq. (53) E_v is generated from E_J in 2nd order RG so that $E_v \sim E_J^2$ initially, while E_v is RG relevant at $t < \frac{1}{2}$, so that its value which is to be used by the variational scheme is more weakly E_J dependent. We assume then $E_v \sim E_J^\kappa$ with $0 < \kappa < 2$. Hence in the $\Delta_0 \neq 0$ phases

$$\begin{aligned} \frac{\partial(z + \Delta_0)}{\partial E_J} &= \frac{\kappa(z + \Delta_0)}{E_J(1 - 2t)} \\ \frac{\partial z}{\partial E_J} &= \frac{(2 - \kappa)}{(1 - 2s)E_J} \\ \langle \cos b \rangle &= -\kappa(1 - 2t)\frac{z + \Delta_0}{z_{bare}} + (1 - \frac{1}{2}\kappa)\frac{z}{z_{bare}} \end{aligned} \quad (71)$$

where $z_{bare} = E_J/Td$ is the bare value of z . For the $\Delta_0 = 0$ phase

$$\begin{aligned} \frac{\partial z}{\partial E_J} &= \frac{z}{(1 - t - s)E_J} \\ \langle \cos b \rangle &= \frac{z}{z_{bare}} \end{aligned} \quad (72)$$

so that at $T = s = 0$ the order is maximal, $\langle \cos b \rangle = 1$.

These results show that the JG order produces a negative contribution to $\langle \cos b \rangle$ so that when crossing a depinning line $\langle \cos b \rangle$ is enhanced by the $\sim \kappa$ terms in Eq. (71). Since Δ_0 is continuous, the jump at depinning is $\kappa(\frac{3}{2} - 2t)z/z_{bare}$. As discussed in section III, the depinning in the lower part of Fig. 1 is not a strict phase transition, but rather a

crossover line, hence we expect a smeared jump of $\langle \cos b \rangle$. An observation of a $\langle \cos b \rangle$ enhancement when crossing the lower depinning line at $T \approx T_0$ ($B < B_0$) would be a clear signature that depinning relates to JG order. The actual enhancement depends on κ , for which we do not have a precise derivation.

Near the decoupling transitions, the presence of anharmonic regimes, shown in section IV, lead to an apparent jump in $\langle \cos b \rangle$. This jump relates to the z terms in (71) and also depends on the fluctuation contribution which is considered next.

We proceed to evaluate fluctuation contribution when $\langle \cos b \rangle$ is small. As shown by Koshelev¹⁴ the local $\langle \cos b_n(r) \rangle$ is finite even at high temperatures, e.g. above the decoupling transition. A high temperature expansion yields¹⁴

$$\begin{aligned} \langle \cos b_n(r) \rangle &= (E_J/2T) \int d^2r \exp[-A(r)] \\ A(r) &= \sum_{\mathbf{q}, k} (1 - \cos \mathbf{q} \cdot \mathbf{r}) \langle |b^\alpha(\mathbf{q}, k)|^2 \rangle. \end{aligned} \quad (73)$$

For $r^2 > 1/q_u^2$ we can use the form (45) with z replaced by a cutoff $c(k)/r^2$ while for $r < 1/q_u$ we expand $1 - \cos \mathbf{q} \cdot \mathbf{r} \rightarrow \frac{1}{4}q^2r^2$, hence

$$\begin{aligned} A(r) &= 4(s+t) \ln(q_u r) \quad r > 1/q_u \\ &= \frac{1}{2}(s+t)q_u^2 r^2 \quad r < 1/q_u. \end{aligned} \quad (74)$$

The larger contribution at $s+t \gg \frac{1}{2}$ (where (73) is valid) comes from $r < 1/q_u$ which yields $\int_0^{1/q_u} \exp[-A(r)] d^2r = 2\pi/[(s+t)q_u^2]$, hence in terms of the multicritical point coordinates (up to $\ln B$ terms)

$$\langle \cos b \rangle \approx \frac{\pi E_J \lambda_{ab}^2}{2 \ln(a/d)} \cdot \frac{B_0 T_0}{BT(T+T_0)} \quad (75)$$

A $1/BT$ dependence has been obtained by Koshelev¹⁴ with a weakly temperature dependent prefactor for an XY model, i.e. infinite λ_{ab} model. Data on BSCCO¹³ has shown that $\langle \cos \tilde{b}_n(r) \rangle \sim B^{-0.8} T^{-1}$ in reasonable agreement with the $1/BT$ form. The present result shows that in fact the $1/BT$ form is valid in the disorder dominated regime, i.e. $T < T_0$, though in general the fluctuation term yields $\omega_{pl}^2 \sim 1/[BT(T+T_0)]$.

While (75) is not expected to hold near decoupling, we expect a positive fluctuation term to compensate the negative contribution of the JG order. Thus the forms (71,72) can be used for the jumps of $\langle \cos b \rangle$ across depinning or decoupling, while (73) is valid in the high temperature or high field regime where $\langle \cos b \rangle$ is small.

VI. DISCUSSION

The present work demonstrates the JG order parameter as well as decoupling. We discuss now our proposal for each of the 4 transition lines emanating from the multi-critical point (Fig. 2) and compare with experimental data.

Consider first the decoupling transition within the JG phase at $B = B_0$, $T < T_0$. We have shown that RSB methods are suspect within a narrow region near decoupling, where usual elasticity is ill defined (Fig. 3). RSB identifies this as a $\ln^2 z$ divergence in A_α which renormalizes z (Eq. 24). This can be thought of as a disorder term $\sim s_{eff} \ln z$ with a diverging s_{eff} . The consequence is an apparent discontinuity, or even an intrinsic 1st order transition, driven by disorder.

This decoupling transition is consistent with the main features of the second peak transition: (i) decoupling field being weakly T dependent^{1,2,3,4}, (ii) decoupling field decreasing with impurity concentration², (ii) an apparent jump in the critical current and^{1,2,3,4,8,9,10,11}

(iv) a jump in the Josephson plasma resonance^{15,16}. The anharmonic region near decoupling leads to an apparent reduction in c_{44} . The reduction in c_{44} and the resulting reduction in domain sizes account qualitatively for the enhanced j_c . We do not attempt a quantitative fit; in fact, the measured magnetization changes (and inferred j_c) at the second peak decrease with temperature due to the strongly temperature dependent relaxation rates⁴⁶, approaching the much smaller equilibrium magnetizations.

The nature of the phase at fields above the second peak line has not been conclusively settled. This work proposes that it is a BG phase where the domain sizes have been reduced by $\sqrt{\epsilon} = a^2/(4\pi\sqrt{2}\lambda_{ab}^2)$. Experimentally, the smooth connection with the 1st order line⁵ suggests that it is a melting line. However, decoration data¹² on $NbSe_2$ show that the topology of the vortex structure is weakly affected by the transition.

Consider next the decoupling line at $T > T_0$. This corresponds to the 1st order transition, which is considered as a melting line^{1,5}. However, neutron data⁷ has shown a reentrant behavior in the $600 - 10^3 G$ range with positional

correlations increasing with temperature. It is possible then that near the multi-critical point the 1st order line is a decoupling line. At higher temperatures decoupling then merges into a melting line.

The 3rd transition line is the crossover of the JG order at $T = T_0$, $B < B_0$ into a weaker JG at $T > T_0$. A depinning line which is almost vertical at $T \approx T_0$ was indeed observed^{17,18,19}. The observed line is frequency dependent¹⁷, consistent with it being a crossover line. At this line we expect an enhancement of the Josephson plasma resonance, which can then identify the role of JG in this transition.

The final 4th line is a depinning line at $T = B_0 T_0 / B$, $B > B_0$ in qualitative agreement with a stronger B dependence^{17,19} of depinning at $B > B_0$. This line is more difficult to detect since the Josephson plasma frequency should vary smoothly. In the decoupled phases (with or without JG order), where $\langle \cos b \rangle$ is small, we expect the fluctuation form Eq. (75).

We have assumed throughout that our transition lines are well below melting. We expect that for some of the layered superconductors this assumption fails. In particular in low T_c compounds such as⁸ NCCO or¹² $NbSe_2$ the temperature T_0 would be too close to T_c , hence the depinning lines, as well as the multicritical point, are probably not realized.

In conclusion, we have found a phase diagram which is remarkably close to the experimental one^{1,2,3,4,17,19}, having a multicritical point and providing a fundamental interpretation of both the second peak transition and the more recently observed depinning transitions.

Acknowledgments: We thank E. Zeldov, D. T. Fuchs for most valuable and stimulating discussions. This research was supported by THE ISRAEL SCIENCE FOUNDATION founded by the Israel Academy of Sciences and Humanities.

APPENDIX A: BRAGG AND JOSEPHSON GLASSES

This section studies nonlinearities due to both disorder and Josephson coupling leading to two glass order parameters – the Josephson glass (JG) and the Bragg glass (BG); the non-singular phase is neglected. In particular an equivalent term to the integral $I(z)$ (Eq. 46) is identified and is shown to be convergent at $k \rightarrow 0$.

We consider the full Hamiltonian Eq. (22), which by neglecting the nonsingular phase becomes

$$\begin{aligned} \mathcal{H}/T = & \frac{1}{2} \sum_{\mathbf{q}, k, \alpha} (c' \frac{q^4}{k_z^2} + c(k)q^2) |b^\alpha(\mathbf{q}, k)|^2 - \frac{E_J}{T} \sum_{n, \alpha} \int d^2 r \cos b_n^\alpha(\mathbf{r}) \\ & - \frac{E_v}{T} \sum_{n, \alpha \neq \beta} \int d^2 r \cos[b_n^\alpha(\mathbf{r}) - b_n^\beta(\mathbf{r})] - \frac{g}{a^2} \sum_{\alpha \neq \beta, n} \int d^2 r \cos[\mathbf{Q} \cdot (\mathbf{u}^{n, \alpha}(\mathbf{r}) - \mathbf{u}^{n, \beta}(\mathbf{r}))] \end{aligned} \quad (\text{A1})$$

The average of the disorder term over the variational Hamiltonian (23) \mathcal{H}_0 yields

$$\langle \cos[\mathbf{Q} \cdot (\mathbf{u}^{n, \alpha}(\mathbf{r}) - \mathbf{u}^{n, \beta}(\mathbf{r}))] \rangle = \exp\left\{-\frac{a^2}{2d^2} \sum_{\mathbf{q}, k} \frac{q^2}{k_z^2} [G_{\alpha\alpha}(q, k) - G_{\alpha\beta}(q, k)]\right\}. \quad (\text{A2})$$

We assume for simplicity a square lattice, $Q = 2\pi/a$, otherwise a factor $(aQ/2\pi)^2$ is needed in the exponent. The variational equation for $G_{\alpha\beta}^{-1}(q, k)$, Eq. (27), has now an additional self energy term $\sigma_{\alpha\beta}^{(1)}$ which allows for an additional RSB. Written as an equation for matrices in replica space, e.g. \hat{G} , we have

$$\hat{G}^{-1}(q, k) = (c' \frac{q^4}{k_z^2} + c(k)q^2 + z)\hat{I} - \hat{\sigma}_2 - \frac{q^2}{k_z^2} \hat{\sigma}_1. \quad (\text{A3})$$

When $(\hat{\sigma}_1)_{\alpha\beta} = 1$, i.e. no RSB, the previous form (27) is recovered. The variational \mathcal{F}_{var} (26) has now a term $\sim \exp[-\frac{1}{2}B_{\alpha\beta}^{(1)}]$ (instead of the s_0 term) where

$$B_{\alpha\beta}^{(1)} = \frac{a^2}{d^2} \sum_{\mathbf{q}, k} \frac{q^2}{k_z^2} [G_{\alpha\alpha}(q, k) - G_{\alpha\beta}(q, k)]. \quad (\text{A4})$$

The variation of this term identifies

$$\sigma_{\alpha\beta}^{(1)} = \frac{g}{d^3} [e^{-\frac{1}{2}B_{\alpha\beta}^{(1)}} - \delta_{\alpha\beta} \sum_{\gamma} e^{-\frac{1}{2}B_{\alpha\gamma}^{(1)}}] \quad (\text{A5})$$

while $\sigma_{\alpha\beta}^{(2)}$ and $B_{\alpha\beta}^{(2)}$ have the previous forms (25, 29). In the hierarchical scheme G^{-1} is represented by $[\tilde{a}, a(u)]$ which are now given by

$$\begin{aligned}\tilde{a} &= c' \frac{q^4}{k_z^2} + c(k)q^2 + z - \tilde{\sigma}_2 - \tilde{\sigma}_1 \frac{q^2}{k_z^2} \\ a(u) &= -\sigma_2(u) - \sigma_1(u) \frac{q^2}{k_z^2}.\end{aligned}\tag{A6}$$

The JG and BG order parameters which measure the degree of RSB are $\Delta_1(u), \Delta_2(u)$, respectively, where $\Delta_i(u) = u\sigma_i(u) - \int_0^u \sigma_i(v)dv$, $i = 1, 2$. Using the inversion (32) we can write

$$\frac{1}{2}B_i(u) = \frac{g_i(u)}{u} - \int_u^1 \frac{g_i(v)}{v^2} dv \quad i = 1, 2\tag{A7}$$

where

$$\begin{aligned}g_1(u) &= \frac{a^2}{2d^2} \sum_{\mathbf{q}, k} [c'q^2 + c(k)k_z^2 + (z + \Delta_2(u))\frac{k_z^2}{q^2} + \Delta_1(u)]^{-1} \\ g_2(u) &= \sum_{\mathbf{q}, k} [c' \frac{q^4}{k_z^2} + c(k)q^2 + z + \Delta_2(u) + \Delta_1(u)\frac{q^2}{k_z^2}]^{-1}.\end{aligned}\tag{A8}$$

As in Eq. (39), we find

$$\frac{\Delta'_i(u)}{u} = -\frac{d}{du} \left[\frac{\Delta'_i(u)}{g'_i(u)} \right] \quad i = 1, 2.\tag{A9}$$

Consider first $g_2(u)$ which is dominated by $k \gg q$ so that the c' term produces just the cutoff q_u . The q integration then yields Eq. (38) with $\Delta_c \rightarrow [c(k) + \Delta_1(u)/k_z^2]q_u^2$ in the logarithm. As above, we replace k by π/d in this logarithm since the k integral is dominated by $k \approx \pi/d$ due to the significant softening of $c(k)$ near $k = \pi/d$. Hence the form $g_2(u) \sim \ln[z + \Delta_2(u)]$ is maintained and the solution, as in (40) is a one step function at $u = 2t$.

To solve the equation for $\Delta_1(u)$ we simplify the form of $c(k)$ as

$$\begin{aligned}c(k) &= c(0) \equiv c_- \quad k < \frac{1}{a} \\ &= c\left(\frac{\pi}{d}\right) \frac{4}{d^2 k_z^2} \quad k > \frac{1}{a}\end{aligned}\tag{A10}$$

This form captures the significant dispersion of $c(k)$ with $c(\pi/d) \ll c(0)$ and allows analytic treatment of the potentially divergent $k \rightarrow 0$ integrals. The $k > \frac{1}{a}$ integration range in $g_1(u)$ has an integrand

$$[c'q^2 + \Delta_1(u) + c(\pi/d)(4/d^2) + (z + \Delta_2(u))k_z^2/q^2]^{-1}$$

so that $c(\pi/d)(4/d^2) \gg \Delta_1(u)$ provides a cutoff on the q integration, i.e. $g_1(u)$ acquires a term independent of $\Delta_1(u)$. The $k < \frac{1}{a}$ integration has $c(0)/a^2 \gg \Delta_1(u)$ so that after the k integration

$$g_1(u) = \frac{a^2}{8\pi d^2} \int \frac{q^2 dq}{\sqrt{(c'q^2 + \Delta_1(u))(c_-q^2 + z + \Delta_2(u))}} + const.\tag{A11}$$

$\Delta_1(u)$ varies between $\Delta_1(0) = 0$ and $\Delta_1(u_c)$ which depends on the disorder strength (see below); $\Delta(u) = \Delta(u_c)$ is constant at $u > u_c$, being a valid solution of (A9). As the decoupling transition is approached and $z \rightarrow 0$ the q integration in (A11) has distinct forms depending on the ratio of $\Delta_1(u)$ and $c'z/c_-$. When $\Delta_1(u) < c'z/c_-$ the dominant integration range is $\Delta_1(u)/c' < q^2 < z/c_-$ and the result for the derivative is

$$\frac{d}{d\Delta_1} g_1(\Delta_1) = \frac{\alpha'}{\sqrt{z}} \ln \Delta_1 \quad \alpha' = \frac{a^2}{8\pi d^2 c'^{3/2}}.\tag{A12}$$

Substituting in (A9) yields $\Delta_1(u) \approx u\sqrt{z}/\alpha' \ln^2 u$ and with (A7) we obtain $[C_2 = g_1(u=0)]$

$$\begin{aligned}g_1(u) &= C_2 + \frac{u}{\ln u} + O\left(\frac{u}{\ln^2 u}\right) \\ \frac{1}{2}B_1(u) &= C_2 + \ln \ln u + O\left(\frac{1}{\ln u}\right)\end{aligned}\tag{A13}$$

so that $\sigma_1(u) \sim 1/\ln u \rightarrow 0$ at $u \rightarrow 0$. When $\Delta_1(u) > c'z/c(0)$ the dominant integration range is $z/c(0) < \Delta_1(u)/c' < q^2$ so that $z = 0$ can be taken and

$$\frac{d}{d\Delta_1} g_1(\Delta_1) = -\frac{\alpha_-}{\sqrt{\Delta_1}} \quad \alpha_- = \frac{a^2}{8\pi c' c_-^{1/2}}. \quad (\text{A14})$$

Substituting in (A9) yields $\Delta_1(u)$, so that in both regimes we have to leading order in u

$$\begin{aligned} \Delta_1(u) &= \frac{u\sqrt{z}}{\alpha' \ln^2 u} & \Delta_1(u) < z \frac{c'}{c_-} \\ &= \frac{u^2}{4\alpha_-^2} & \Delta_1(u) > z \frac{c'}{c_-}. \end{aligned} \quad (\text{A15})$$

Integrating (A14) and using (A7) for $2\alpha_- \sqrt{c'z/c_-} < u < u_c$,

$$\begin{aligned} g_1(u) &= C_2 - u \\ \frac{1}{2} B_1(u) &= C_2 - \ln \frac{u}{u_c} - u_c \end{aligned} \quad (\text{A16})$$

so that $\sigma_1(u) \sim u$ in this range. We suspect that the solution at $\Delta_1(u) < zc'/C_-$ is significantly modified by the non-singular phase (as indeed found in Appendix B). This is of no concern since anyway the effect of this range on the z equation vanishes (Eq. A20 below).

We finally consider the equation for z by using the inversion formula (32)

$$\begin{aligned} A_\alpha = \int_{\mathbf{q},k} \tilde{G}(q,k) &= \int_{\mathbf{q},k} \frac{1}{c' \frac{q^4}{k_z^2} + c(k)q^2 + z} \left[\frac{\sigma_2(0) + \sigma_1(0) \frac{q^2}{k_z^2}}{c' \frac{q^4}{k_z^2} + c(k)q^2 + z} + 1 \right. \\ &\quad \left. + \int_0^1 \frac{dv}{v^2} \frac{\Delta_2(v) + \Delta_1(v) \frac{q^2}{k_z^2}}{c' \frac{q^4}{k_z^2} + c(k)q^2 + z + \Delta_2(v) + \Delta_1(v) \frac{q^2}{k_z^2}} \right] \end{aligned} \quad (\text{A17})$$

Taking $\sigma_2(0) \sim z$ from section III the $\sigma_2(0)$ term yields a constant, independent of z . Note that without BG order, $\Delta_1(u) = 0$, the one step solution for $\Delta_2(u)$ reproduces the s_0 terms in Eq. (44).

Consider first the range $k < 1/a$ which led to an apparent divergence in section III. For small v , where the v integral may diverge, we take $\Delta_2(v) = 0$ so that

$$A_1 = \int_0^1 \frac{dv}{v^2} \int_{\mathbf{q}} \int_{k < 1/a} k^2 \left[\frac{1}{c'q^4 + (c_-q^2 + z)k^2} - \frac{1}{c'q^4 + (c_-q^2 + z)k^2 + \Delta_1(u)q^2} \right] \quad (\text{A18})$$

Performing the k integral leads to a $[c_-q^2 + z]^{-3/2}$ factor, which amounts to a lower cutoff $\sqrt{z/c_-}$,

$$A_1 = \int \frac{dv}{4\pi c_-^{3/2} v^2} \int_{\sqrt{z/c_-}} dq [-\sqrt{c'} + \frac{1}{q} \sqrt{\Delta_1(v) + c'q^2}] \quad (\text{A19})$$

For $\Delta_1(v) < zc'/c_-$ one can expand in $\Delta_1(v)$, which from (A15) yields a term

$$\int_0^{\sim \sqrt{z}} \frac{dv}{v^2} \frac{v}{\ln^2 v} \sim \frac{1}{\ln z} \rightarrow 0 \quad z \rightarrow 0. \quad (\text{A20})$$

For the v integration range where $\Delta_1(v) > zc'/c_-$, which exists if $\Delta_1(u_c) > zc'/c_-$, we have

$$A_1 = \frac{1}{4\pi c_-^{3/2}} \left[\int_{\sim \sqrt{z}} \frac{dv}{2v^2} \sqrt{\Delta_1(v)} \ln \frac{4c_- \Delta_1(v)}{c'z} - \frac{1}{4\alpha_-} \ln z \right] = \frac{1}{64\pi \alpha_- c_-^{3/2}} [\ln^2 z + O(\ln z)]. \quad (\text{A21})$$

The second contribution to A_α is from the range $k > 1/a$ where $c(k)k_z^2 \approx \text{constant}$ provides a cutoff in the A_α integrations, hence $\Delta_1(v)$ can be neglected in the denominator, leading to

$$A_2 = \int_{k > 1/a} \int_{\mathbf{q}} \frac{q^2}{k_z^2 [c(k)q^2 + z]^2} \int_0 \frac{dv}{v^2} \Delta_1(v) \quad (\text{A22})$$

Identifying $s_0 = \int_0^{\frac{dv}{v^2}} \Delta_1(v)$ we obtain the form (50) for $I(z)$, i.e. $A_2 = -2s \ln z$. Collecting both terms we finally have

$$A_\alpha = \frac{\pi d^2 \lambda_{ab}^2}{a^4} \ln^2 z - 2s \ln z + O(\ln z) \quad (\text{A23})$$

where additional $\ln z$ terms involve $\Delta_2(v)$ and t as in 47, 48).

We proceed to identify $\Delta_1(u)$, which determines the BG domain size, and to examine the condition $\Delta_1(u_c) > zc'/c_-$ necessary for the appearance of the $\ln^2 z$ term in (A23). Eqs. (A5, A16) yield for the range $2\alpha\sqrt{c'z/c_-} < u < u_c$,

$$\sigma_1(u) = \frac{g}{d^3} \frac{u}{u_c} e^{-C_2+u_c}. \quad (\text{A24})$$

The definition $\Delta_1(u) = u\sigma_1(u) - \int_0^u \sigma_1(v)dv$ then leads to

$$\Delta_1(u_c) = \frac{g}{2d^3} u_c e^{-C_2+u_c} \quad (\text{A25})$$

C_2 is a Debye Waller factor which is small by the assumption of being well below melting, $T/\tau \ll 1$. Comparing with (A15) we identify $u_c \approx 10^4 s T d^2 \xi_0^4 / \lambda_{ab}^2 a^4 \ll 1$ and $\Delta_1(u_c) \approx \alpha_- (g/d^3)^2$.

$\Delta_1(u_c)$ is related to the BG domain size in the axis perpendicular to the layers $L_{BG}^- = \sqrt{c_-/\Delta_1(u_c)}$ or in the ab plane $R_{BG}^- = \sqrt{c'/\Delta_1(u_c)}$, as identified by the q, k cutoffs in $g_1(u)$ (Eq. A8), or by evaluating displacement correlations²². Hence

$$R_{BG}^- \approx \frac{10^{-4} \lambda_{ab}^3 a^3}{sd\xi_0^4} \quad (\text{A26})$$

while $L_{BG}^- = R_{BG}^- a / (\lambda_{ab} \sqrt{2\pi})$. These forms are valid close to decoupling [$\Delta_1(u_c) > zc'/c_-$] or in the decoupled phase ($z = 0$). Remarkably, this result of R_{BG} is, up to the 10^{-4} factor, identical to that found from the dimensional analysis Eq. (62) with $\langle u_T^2 \rangle \approx a^2$. We do not attempt to evaluate R_{BG} in the coupled phase with $\Delta_1(u_c) < zc'/c_-$ since then the nonsingular phase, being neglected here, is essential for generating the proper c_{44} . As noted above, for the purpose of decoupling the value of A_α in the $k < 1/a$ range for large z [$zc'/c_- > \Delta_1(u_c)$] is negligible even without the nonsingular phase, as seen in (A20).

The condition $\Delta_1(u_c) > zc'/c_-$, for the appearance of the $\ln^2 z$ in Eq. (A23) can be written in terms of λ_c^R (Eq. 56) with $\sqrt{z/c_-} = 1/\lambda_c^R \sqrt{\epsilon}$,

$$\lambda_c^R > R_{BG}^- / \sqrt{\epsilon} \approx \frac{10^{-3} a \lambda_{ab}^5}{sd\xi_0^2}. \quad (\text{A27})$$

For typical BSCCO or YBCO parameters this implies a renormalized anisotropy of $\lambda_c^R/\lambda_{ab} > 10^5$, i.e. fairly close to decoupling at $z = 0$. Note that $R_{BG}^-/\sqrt{\epsilon}$ can be identified as R_{BG}^+ , the BG domain size in the coupled phase, as shown in Appendix B and section IV.

APPENDIX B: BRAGG GLASS WITH NON-SINGULAR PHASE

We solve here the decoupling transition with nonlinear coupling of disorder (BG effects) and with the non-singular phase. The E_v term of Eq. (22) is neglected, i.e. no JG effects. This describes correctly thermal decoupling, i.e. the line $s + t = 1$ in Fig. 1 where JG is absent within the RSB scheme. To identify the proper \mathcal{H}_0 , we expand the renormalized Josephson coupling $-z \cos[b_n^\alpha(\mathbf{r}) + \theta_n^\alpha(\mathbf{r})] \approx \frac{1}{2} z [b_n^\alpha(\mathbf{r}) + \theta_n^\alpha(\mathbf{r})]^2$ so that with the other Gaussian terms of (16) we have

$$\begin{aligned} \mathcal{H}_0 = \frac{1}{2} \int \frac{d^2 q dk}{(2\pi)^3} [G_f^{-1}(q, k) |\theta^\alpha(q, k)|^2 &+ z |\theta^\alpha(q, k) + b^\alpha(q, k)|^2 + c(q, k) q^2 |b^\alpha(q, k)|^2 \\ &- \frac{q^2}{k_z^2} \sigma_{ab} b^{\alpha*}(q, k) b^\beta(q, k)]. \end{aligned} \quad (\text{B1})$$

Formally, one needs to perform a variation of $\langle \cos[b_n^\alpha(\mathbf{r}) + \theta_n^\alpha(\mathbf{r})] \rangle = \exp[-\frac{1}{2} A_\alpha]$ where

$$A_\alpha = \sum_{\mathbf{q}, k} \langle |\theta^\alpha(q, k) + b^\alpha(q, k)|^2 \rangle \quad (\text{B2})$$

to obtain the z term in (B1). This procedure was also used for decoupling in presence of columnar defects³². We proceed as in the pure case (54) by shifting to

$$\tilde{\theta}^\alpha(q, k) = \theta^\alpha(q, k) + \frac{z}{G_f^{-1}(q, k) + z} b^\alpha(q, k) \quad (\text{B3})$$

which yields

$$\begin{aligned} \mathcal{H}_0 &= \frac{1}{2} \int [(G_f^{-1}(q, k) + z) |\tilde{\theta}^\alpha(q, k)|^2 + G_{\alpha\beta}^{-1}(q, k) b^{\alpha*}(q, k) b^\beta(q, k)] \\ G_{\alpha\beta}^{-1}(q, k) &= [c' \frac{q^4}{k_z^2} + c(k) q^2 + \frac{z q^2}{q^2 + (1 + \lambda_{ab}^2 k_z^2)/(\lambda_c^R)^2}] \delta_{\alpha\beta} - \frac{q^2}{k_z^2} \sigma_{\alpha\beta} \end{aligned} \quad (\text{B4})$$

where the last term corresponds to the B^2 term of c_{44} (Eq. 55) with λ_c replaced by λ_c^R . Note that for $q \gg (1 + \lambda_{ab}^2 k_z^2)^{1/2}/\lambda_c^R$ this reduces to (A3) with $\sigma_2 \rightarrow 0$. A term corresponding to the last term of (55), being $\sim (\lambda_c^R)^{-2}$, is neglected.

We proceed to evaluate $g_1(u)$ with (A8) replaced here by

$$g_1(u) = \frac{a^2}{2d^2} \sum_{\mathbf{q}, k} [c' q^2 + [c(k) + \frac{z}{q^2 + (1 + \lambda_{ab}^2 k_z^2)/(\lambda_c^R)^2}] k_z^2 + \Delta_1(u)]^{-1}. \quad (\text{B5})$$

For $k > 1/a$ $c(k) k_z^2 \gg \Delta_1(u)$ and $g_1(u)$ is Δ_1 independent, as in Appendix A. For $k < 1/a$ two regimes are identified, where the coefficient of the k_z^2 term in (B5) becomes

$$\begin{aligned} c_+ &= c(0) + z(\lambda_c^R)^2 = c_- + \frac{\lambda_{ab}^2 \tau}{4\pi T d^3} \quad q < 1/\lambda_c^R \\ c_- &= c(0) = \frac{a^4 \tau}{2(4\pi d)^3 \lambda_{ab}^2 T} \quad q > 1/\lambda_c^R \end{aligned} \quad (\text{B6})$$

so that $c_+/c_- = 1 + 1/\epsilon \gg 1$ with ϵ defined in (59). This reflects the significant dependence of c_{44} on interchanging the $q \rightarrow 0$ and $1/\lambda_c^R \rightarrow 0$ limits, as discussed in section IV. After the k integration we obtain (replacing A11)

$$g'_1(\Delta_1) = -\frac{a^2}{8\pi d^2} \left[\int_0^{1/\lambda_c^R} \frac{1}{\sqrt{c_+}} + \int_{1/\lambda_c^R} \frac{1}{\sqrt{c_-}} \right] \frac{q dq}{\sqrt{c' q^2 + \Delta_1}} \approx \alpha_\pm / \sqrt{\Delta_1} \quad (\text{B7})$$

where $\alpha_\pm = a^2/(8\pi c' \sqrt{c_\pm})$ with α_+ for $\sqrt{\Delta_1(u)/c'} > 1/\lambda_c^R$ and α_- for $\sqrt{\Delta_1(u)/c'} < 1/\lambda_c^R$. Hence $\Delta_1(u) = u^2/4\alpha_\pm$ and Eqs. (A16, A24) are valid in both α_\pm regimes. Comparing (A25) with $u^2/4\alpha_\pm$ identifies $u_c \approx 2\alpha_\pm g/d^3$ and $\Delta_1(u_c) \approx \alpha_\pm (g/d^3)^2$. The BG scales $R_{BG}^\pm = \sqrt{c'/\Delta_1(u_c)}$ are therefore

$$\begin{aligned} R_{BG}^+ &\approx \frac{10^{-3} a \lambda_{ab}^5}{sd \xi_0^2} \quad R_{BG}^+ < 1/\lambda_c^R \\ R_{BG}^- &\approx \frac{10^{-4} \lambda_{ab}^3 a^3}{sd \xi_0^4} \quad R_{BG}^- > 1/\lambda_c^R \end{aligned} \quad (\text{B8})$$

so that $R_{BG}^+ = \sqrt{\alpha_+/\alpha_-} R_{BG}^- = R_{BG}^-/\sqrt{\epsilon}$. The range $R_{BG}^- < \lambda_c^R < R_{BG}^+$ allows for both length scales and serves as a crossover between the regimes in (B8). The ratio $R_{BG}^+ = R_{BG}^-/\sqrt{\epsilon}$ reflects the change in elastic constants, as in the dimensional argument of section IV. The result (B8) for R_{BG}^- agrees with (A26) in Appendix A.

Renormalization of z requires the sum (B2) which is averaged with respect to \mathcal{H}_0 of (B4)

$$\begin{aligned} A_\alpha &= \sum_{\mathbf{q}, k} |\tilde{\theta}^\alpha(q, k) - \frac{z}{G_f^{-1}(q, k) + z} b^\alpha(q, k) + b^\alpha(q, k)|^2 \\ &= \sum_{\mathbf{q}, k} \left[\frac{1}{G_f^{-1}(q, k) + z} + \left(\frac{z}{G_f^{-1}(q, k) + z} \right)^2 G_{\alpha\alpha}(q, k) \right]. \end{aligned} \quad (\text{B9})$$

The first term is $\approx (T/\tau) \ln z$ and is neglected at $T \ll \tau$. The second term has a factor

$$\frac{z}{G_f^{-1}(q, k) + z} = \frac{q^2}{q^2 + (1 + \lambda_{ab}^2 k_z^2)/(\lambda_c^R)^2} \quad (\text{B10})$$

which for $q < (1 + \lambda_{ab}^2 k_z^2)^{1/2} / \lambda_c^R$ strongly reduces the q integration, while for larger q , A_α becomes

$$A_\alpha = \int'_{\mathbf{q},k} \frac{1}{c' \frac{q^4}{k_z^2} + c(k)q^2 + z} \left[1 + \int_0^1 \frac{dv}{v^2} \frac{\Delta_1(v) \frac{q^2}{k_z^2}}{c' \frac{q^4}{k_z^2} + c(k)q^2 + z + \Delta_1(v) \frac{q^2}{k_z^2}} \right] \quad (\text{B11})$$

where \int' indicates $q > (1 + \lambda_{ab}^2 k_z^2)^{1/2} / \lambda_c^R$. For $k > 1/a$, $c(k)k_z^2 \gg \Delta_1(u)$ provides a cutoff with the result $A_2 = 2s \ln(\Delta_c/z)$ as in Eq. (A22). For $k < 1/a$ the v integral term of (B11) becomes A_1 as in (A18) except for a q cutoff in \int' . The k integration of (A18) produces a cutoff $q > \sqrt{z/c_-} = 1/(\lambda_c^R \sqrt{\epsilon}) \gg (1 + \lambda_{ab}^2 k_z^2)^{1/2} / \lambda_c^R$, hence (A19) is valid. For $\Delta_1(v) < zc'/c_-$

$$\frac{1}{\sqrt{z}} \int_0^{\sim \sqrt{z}} \frac{dv}{v^2} \Delta_1(v) \sim \text{const.} \quad (\text{B12})$$

while for $\Delta_1(v) > zc'/c_-$ (A21) is reproduced. The latter integration range exists if $\Delta_1(u_c) > zc'/c_-$, i.e. $R_{BG}^- < \sqrt{c_-/z} = \lambda_c^R \sqrt{\epsilon}$. Using (B8) we identify the condition for the appearance of the $\ln^2 z$ term as

$$R_{BG}^+ < \lambda_c^R \quad \text{onset of } \ln^2 z \text{ term.} \quad (\text{B13})$$

This is also the condition found in Appendix A (Eq. A27), as well as the condition of section IV, as illustrated in Fig. 3, for the onset of the anharmonic regime.

APPENDIX C: JOSEPHSON GLASS WITH NON-SINGULAR PHASE

In this appendix we extend the solution of section III to include the nonsingular phase. In particular we identify the pinning length R_p in the coupled phase and show that it coincides with (62) (with $\langle u_T^2 \rangle \approx \xi_0^2$), up to a numerical prefactor. Since disorder is linearized, we do not expect to derive BG domain sizes. Also the integral $I(z)$ is reconsidered.

Consider then Eq. (12) with the pure part replaced by Eq. (16). The harmonic part can be written as

$$\begin{aligned} G_f^{-1}(q, k) |\tilde{b}^\alpha(q, k) - b^\alpha(q, k)|^2 + [c(q, k)q^2 \delta_{\alpha\beta} - s_0 \frac{q^2}{k_z^2}] b^\alpha(q, k) b^{\beta*}(q, k) \\ = G_f^{-1}(q, k) |\tilde{b}^\alpha(q, k)|^2 + d^\alpha B_{\alpha\beta}^{-1}(q, k) d^{\beta*}(q, k) - G_f^{-2}(q, k) B_{\gamma\alpha} \tilde{b}^\gamma(q, k) \tilde{b}^{\alpha*}(q, k) \end{aligned} \quad (\text{C1})$$

where

$$\begin{aligned} d^\alpha(\mathbf{q}, k) &= b^\alpha(\mathbf{q}, k) - B_{\gamma,\alpha}(q, k) G_f^{-1}(q, k) \tilde{b}^\alpha(\mathbf{q}, k) \\ B_{\alpha,\beta}^{-1}(q, k) &= G_f^{-1}(q, k) \alpha(q, k) \delta_{\alpha,\beta} - s_0 \frac{q^2}{k_z^2} \\ \alpha(q, k) &= 1 + G_f(q, k) c(q, k) q^2. \end{aligned} \quad (\text{C2})$$

The resulting replicated Hamiltonian is

$$\begin{aligned} \mathcal{H}^{(2)}/T &= \frac{1}{2} \sum_{\mathbf{q}, k; \alpha, \beta} B_{\alpha,\beta}^{-1} d^\alpha(\mathbf{q}, k) d^{\beta*}(\mathbf{q}, k) + \frac{1}{2} \left[\frac{c(q, k)}{\alpha(q, k)} q^2 \delta_{\alpha,\beta} - \frac{s_0 q^2}{\alpha^2(q, k) k_z^2} \right] \tilde{b}^\alpha(\mathbf{q}, k) \tilde{b}^{\beta*}(\mathbf{q}, k) \\ &\quad - \frac{E_J}{T} \sum_{n; \alpha} \int d^2 r \cos \tilde{b}_n^\alpha(\mathbf{r}) - \frac{E_v}{T} \sum_{n; \alpha \neq \beta} \int d^2 r \cos [\tilde{b}_n^\alpha(\mathbf{r}) - \tilde{b}_n^\beta(\mathbf{r})]. \end{aligned} \quad (\text{C3})$$

The effect of the nonsingular phase on our previous Hamiltonian Eq. (12) of section II is to replace $c(q, k) \rightarrow c(q, k)/\alpha(q, k)$ and $s_0 \rightarrow s_0/\alpha^2(q, k)$. From the definition in Eq. (C2) we find that $\alpha(q, k) - 1$ is either $\sim q^2$ or $\sim k^2$ and is small except when

$$\begin{aligned} \alpha(q, k) - 1 &= \epsilon \quad k < 1/\lambda_{ab}, q < ka/\lambda_{ab} \\ &= \frac{a^2}{16\pi\lambda_{ab}^2} \quad k < 1/\lambda_{ab}, q > ka/\lambda_{ab} \end{aligned} \quad (\text{C4})$$

This behavior is sufficient to eliminate the $k \rightarrow 0$ divergence of $I(z)$ (leading to $\sim 1/\sqrt{z}$) as shown below.

We proceed to evaluate the fluctuations in $u^{tr}(\mathbf{q}, k)$ and identify the scale R_p . From eq. (C2)

$$\langle |u_T(\mathbf{q}, k)|^2 \rangle = (2\pi d^2)^{-2} \frac{q^2}{k_z^2} [\langle d^\alpha(\mathbf{q}, k) d^{\alpha*}(\mathbf{q}, k) \rangle + G_f^{-2}(q, k) B_{\gamma\alpha}(q, k) B_{\gamma'\alpha}(q, k) G_{\alpha\beta}(q, k)]. \quad (C5)$$

Here $G_{\alpha\beta}(q, k) = \langle \tilde{b}_\gamma(\mathbf{q}, k) \tilde{b}_{\gamma'}^*(\mathbf{q}, k) \rangle$ is the solution from section III, and in the replica limit

$$\begin{aligned} \sum_{\gamma\gamma'} G_{\gamma\gamma'}(q, k) &\rightarrow 0 \\ \sum_{\gamma} G_{\alpha\gamma}(q, k) &\rightarrow [\frac{c(q, k)}{\alpha(q, k)} q^2 + z]^{-1} \end{aligned} \quad (C6)$$

where terms involving Δ_0 cancel. Hence

$$\begin{aligned} \langle |u_T(\mathbf{q}, k)|^2 \rangle = & (2\pi d^2)^{-2} \frac{q^2}{k_z^2} [B_{\alpha\alpha}(q, k) + \frac{G_f^{-2}(q, k)}{(G_f^{-1}(q, k) + c(q, k)q^2)^2} \tilde{G}(q, k) \\ & + \frac{2s_0 q^2 / k_z^2}{(G_f^{-1}(q, k) + c(q, k)q^2)^3} \frac{G_f^{-2}(q, k)}{\frac{c(q, k)}{\alpha(q, k)} q^2 + z}]. \end{aligned} \quad (C7)$$

With some straightforward algebra,

$$\begin{aligned} \langle |u_T(\mathbf{q}, k)|^2 \rangle = & (2\pi d^2)^{-2} \frac{q^2}{k_z^4} [s_0 q^2 G_f(\mathbf{q}, k) \alpha^{-1}(\mathbf{q}, k) \left(c(\mathbf{q}, k) q^2 + \frac{G_f^{-1}(\mathbf{q}, k) z}{G_f^{-1}(\mathbf{q}, k) + z} \right)^{-1} \\ & + \frac{s_0}{c(\mathbf{q}, k) \alpha^2(\mathbf{q}, k)} \left(\frac{c(\mathbf{q}, k)}{\alpha(\mathbf{q}, k)} q^2 + z \right)^{-1}] + \dots \end{aligned} \quad (C8)$$

where \dots stands for terms which converge in (\mathbf{q}, k) integration. Note the term $G_f^{-1}(\mathbf{q}, k) z / [G_f^{-1}(\mathbf{q}, k) + z]$ which depends on the order of $q \rightarrow 0$ and $z \rightarrow 0$ limits; this limit dependence leads to the apparent discontinuity in c_{44} as discussed in section IV. For $z \neq 0$ and small q , i.e. $G_f^{-1}(\mathbf{q}, k) \ll z$ the first term in Eq. (C8) dominates, leading to

$$\langle |u_T(\mathbf{q}, k)|^2 \rangle \approx \frac{4\pi^2 s_0 T^2}{a^8 [c_{44} k^2 + c_{66} q^2]^2} \quad q < 1/\lambda_c^R \quad (C9)$$

where c_{44} is from Eq. (57) and the condition $G_f^{-1}(\mathbf{q}, k) \ll z$ is written in terms of λ_c^R (Eq. 56). The correlations at distance r parallel to the layers are then

$$\langle [u_T(r) - u_T(0)]^2 \rangle \approx \frac{4d^2 s_0 T^2}{a^4 c_{44}^{1/2} c_{66}^{3/2}} r \equiv \xi_0^2 \frac{r}{R_p}. \quad (C10)$$

The last equality defines the pinning length R_p where the fluctuations become of order ξ_0^2 . This result for R_p (up to a numerical prefactor) is the same as the one obtained from Eq. (62) with $\langle u_T^2 \rangle \approx \xi_0^2$.

In the decoupled phase with $z = 0$ the second term in Eq. (C8) dominates. To leading order in ϵ the result is identical to Eq. (C10) except that c_{44} is replaced by its $z = 0$ value Eq. (58), i.e. the pinning length is reduced.

Consider next the integral $I(z)$. As noted below Eq. (C3) the nonsingular phase leads to the replacements $c(q, k) \rightarrow c(q, k)/\alpha(q, k)$ and $s_0 \rightarrow s_0/\alpha^2(q, k)$ so that Eq. (46) becomes

$$I(z) = \int \frac{dq^2 dk}{k_z^2 c(q, k) \alpha(q, k)} \frac{1}{[c(q, k)/\alpha(q, k)] q^2 + z}. \quad (C11)$$

In the range $1/a < k < \pi/d$ with $\alpha(q, k) \approx 1$ the q^2 term in $c(q, k)$ amounts to a cutoff q_u^2 (defined below (36)) leading to $I_0(z)$ (49). In the range $1/\lambda_{ab} < k < 1/a$ we have $c(q, k) = c(0)(1 + 2\pi\lambda_{ab}^2 q^2/a^2 k^2)$ and $\alpha(q, k) \approx 1$. The singularity in z which we wish to identify, is exhibited by $q \rightarrow 0$, hence $c(q, k) \approx c(0) = c_-$ leads to the first correction

$$I_1(z) = -\frac{2\lambda_{ab}}{c_-^2} \ln z + const. \quad (C12)$$

In the range $k < 1/\lambda_{ab}$ we have two terms

$$\begin{aligned} I_2(z) &= 2 \int_0^{1/\lambda_{ab}} \frac{dk}{k^2 c_-} \int_0^{\lambda_{ab} k/a} \frac{dq^2}{[1 + \frac{2\pi\lambda_{ab}^2 q^2}{a^2 k^2}][c_- q^2 (1 + \frac{2\pi\lambda_{ab}^2 q^2}{a^2 k^2}) + z]} \\ I_3(z) &= 2 \int_0^{1/\lambda_{ab}} \frac{dk}{k^2 c''} \int_{\lambda_{ab} k/a}^{1/a} \left(\frac{16\pi\lambda_{ab}^2 k^2}{a^2 q^2}\right)^2 \frac{dq^2}{c'' q^2 + z} \end{aligned} \quad (C13)$$

where $c'' = (32\pi^2\lambda_{ab}^4/a^4)c_-$ is due to the finite effect of $c(q, k)/\alpha(q, k)$ when $q > \lambda_{ab}k/a$, $k < 1/\lambda_{ab}$. In $I_2(z)$ the q^4 term replaces the q^2 cutoff as ak/λ_{ab} leading to

$$I_2(z) = \frac{a}{\lambda_{ab}^2 c_-^2} \sqrt{\frac{c_-}{z}} + \frac{2\lambda_{ab}}{c_-^2} \ln z + \text{const.} \quad (C14)$$

while

$$I_3(z) = \frac{(8\pi)^3 \lambda_{ab}}{3ac''^2} \sqrt{\frac{c''}{z}} \quad (C15)$$

is smaller than the 1st term of (C14). We conclude then

$$I(z) = \frac{a}{\lambda_{ab}^2 c_-^2} \sqrt{\frac{c(0)}{z}} + 2s \ln \frac{\Delta_c}{z} + \text{const.} \quad (C16)$$

The effect of the $1/\sqrt{z}$ term is significant, in terms of λ_c^R (Eq. 56) if

$$\frac{\lambda_c^R}{\lambda_{ab}} > \frac{\sqrt{2}\lambda_{ab}^2 a}{4d^2 \ln^2(a/d)} \approx 10^4 \quad (C17)$$

for BSCCO parameters; with bare anisotropy of $\lambda_c/\lambda_{ab} \approx 50$ one needs to be fairly close to the transition to have an effect from the $1/\sqrt{z}$ term. Note that nonlinear coupling of disorder, i.e. BG formulation, is much more efficient in reducing the $I(z)$ singularity, as shown in Appendices A and B.

-
- ¹ For a review see P. H. Kes, J. Phys. I France **6**, 2327 (1996).
² B. Khaykovich, M. Konczykowski, E. Zeldov, R. A. Doyle, D. Majer, P. H. Kes and T. W. Li, Phys. Rev. B, **56**, R517 (1997); Czech. J. Phys. **46-S6**, 3218 (1996).
³ B. Khaykovich, E. Zeldov, D. Majer, T. W. Li, P. H. Kes, and M. Konczykowski, Phys. Rev. Lett. **76**, 2555 (1996).
⁴ K. Deligiannis, P. A. J. de Groot, M. Oussena, S. Pinfold, R. Langan, R. Gagnon and L. Taillefer, Phys. Rev. Lett. **79**, 2121 (1997).
⁵ N. Avraham, B. Khaykovich, Y. Myasoedov, M. Rappaport, H. Shtrikman, D. E. Feldman, T. Tamegai, P. H. Kes, M. Li, M. Konczykowski, K. van der Beek and E. Zeldov, Nature **411**, 451 (2001).
⁶ R. Cubitt, Nature **365**, 407 (1993).
⁷ E. M. Forgan et al., Czech. J. Phys. **46-suppl. S3**, 1571 (1996).
⁸ D. Giller, A. Shaulov, R. Prozorov, Y. Abulafia, Y. Wolfus, L. Burlachkov, Y. Yeshurun, E. Zeldov, V. M. Vinokur, J. L. Peng and R. L. Greene, Phys. Rev. Lett. **79**, 2542 (1997).
⁹ M. J. Higgins and S. Bhattacharya, Physica C **232**, 232 (1996).
¹⁰ A. C. Marley, M. J. Higgins and S. Bhattacharya, Phys. Rev. Lett. **74**, 3029 (1995).
¹¹ Y. Bruynseraede et al., Phys. Scr. **T42**, 37 (1992).
¹² Y. Fasano, M. Menghini, F. de la Cruz, Y. Paltiel, Y. Myasoedov, E. Zeldov, M. J. Higgins and S. Bhattacharya, Phys. Rev. B **66**, 020512 (2002).
¹³ Y. Matsuda, M. B. Gaifullin, K. I. Kumagai, M. Kosugi and K. Hirata, Phys. Rev. Lett. **78**, 1972 (1997).
¹⁴ A. E. Koshelev, Phys. Rev. Lett. **77**, 3901 (1996).
¹⁵ T. Shibauchi, T. Nakano, M. Sato, T. Kisu, N. Kameda, N. Okuda, S. Ooi, and T. Tamegai, Phys. Rev. Lett. **83**, 1010 (1999).
¹⁶ M. B. Gaifullin, Y. Matsuda, N. Chikumoto, J. Shimoyama and K. Kishio, Phys. Rev. Lett. **84**, 2945 (2000).
¹⁷ D. T. Fuchs, E. Zeldov, M. Rappaport, T. Tamegai, S. Ooi and H. Shtrikman, Nature **391**, 373 (1998); D. T. Fuchs, E. Zeldov, T. Tamegai, S. Ooi, M. Rappaport and H. Shtrikman, Phys. Rev. Lett. **80**, 4971 (1998).

- ¹⁸ Y. Kopelevich, A. Gupta and P. Esquinazi, Phys. Rev. Lett. **70**, 666 (1993).
- ¹⁹ C. D. Dewhurst and R. A. Doyle, Phys. Rev. B **56**, 10832 (1997).
- ²⁰ For a review see G. Blatter, M. V. Feigel'man, V. B. Geshkenbein, A. I. Larkin and V. M. Vinokur, Rev. Mod. Phys. **66**, 1125 (1995).
- ²¹ A. I. Larkin and Y. N. Ovchinnikov, J. Low Temp. Phys. **34**, 409 (1979).
- ²² T. Giamarchi and P. Le Doussal, Phys. Rev. B **52**, 1242 (1995).
- ²³ T. Nattermann, Phys. Rev. Lett. **64**, 2454 (1990); J. Kierfeld, T. Nattermann and T. Hwa, Phys. Rev. B **55**, 626 (1997) .
- ²⁴ D. Carpentier, P. Le Doussal and T. Giamarchi, Europhys. Lett. **35**, 397 (1996).
- ²⁵ A. Golub and B. Horovitz, Europhys. Lett. **39**, 79 (1997).
- ²⁶ P. Olsson and S. Teitel, Phys. Rev. Lett. **87**, 137001 (2001).
- ²⁷ Y. Nonomura and X. Hu, Phys. Rev. Lett. **86**, 5140 (2001).
- ²⁸ C. J. Olson, C. Reichardt, R. T. Scalettar, G. T. Zimányi and N. Grønbech-Jensen, Physica C **384** 143 (2003).
- ²⁹ L. I. Glazman and A. E. Koshelev, Physica C **173**, 180 (1991).
- ³⁰ L. L. Daemen, L. N. Bulaevskii, M. P. Maley and J. Y. Coulter, Phys. Rev. Lett. **70**, 1167 (1993).
- ³¹ A. E. Koshelev, L. I. Glazman and A. I. Larkin, Phys. Rev. B **53**, 2786 (1996).
- ³² A. Morozov, B. Horovitz and P. Le Doussal, Phys. Rev. B **67**, 140505(R) (2003).
- ³³ M. J. W. Dodgson, V. B. Geshkenbein and G. Blatter, Phys. Rev. Lett. **83**, 5358 (1999).
- ³⁴ B. Horovitz and P. Le Doussal, Phys. Rev. Lett. **84**, 5395 (2000).
- ³⁵ E. Frey, D. R. Nelson and D. S. Fisher, Phys. Rev. B **49**, 9723 (1994).
- ³⁶ M. C. Marchetti and L. Radzihovsky, Phys. Rev. B **59**, 12001 (1999).
- ³⁷ R. Goldin and B. Horovitz (preceding companion article).
- ³⁸ B. Horovitz and T. R. Goldin, Phys. Rev. Lett. **80**, 1734 (1998).
- ³⁹ B. Horovitz, Phys. Rev. B **60**, R9939 (1999).
- ⁴⁰ L. I. Glazman and A. E. Koshelev, Phys. Rev. B **43**, 2835 (1991).
- ⁴¹ A. Sudbø and E. H. Brandt, Phys. Rev. Lett. **66**, 1781 (1996).
- ⁴² T. R. Goldin and B. Horovitz, Phys. Rev. B **58**, 9524 (1998).
- ⁴³ B. Horovitz and A. Golub, Phys. Rev. B **55**, 14499 (1997); Phys. Rev. B **57**, 656(E) (1998).
- ⁴⁴ S. Scheidl and M. Lehnert, Phys. Rev. B **58**, 8667 (1998).
- ⁴⁵ M. Mézard and G. Parisi, J. Phys., **1**, 809 (1991).
- ⁴⁶ Y. Yeshurun, N. Bontemps, L. Burlachkov and A. Kapitulnik, Phys. Rev. B **49**, 1548 (1994).